TRIUMF

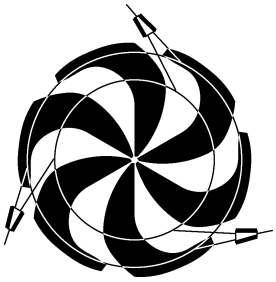

ANNUAL REPORT
SCIENTIFIC ACTIVITIES
2004

ISSN 1492-417X

CANADA'S NATIONAL LABORATORY FOR PARTICLE AND NUCLEAR PHYSICS

OPERATED AS A JOINT VENTURE

MEMBERS:

THE UNIVERSITY OF ALBERTA
THE UNIVERSITY OF BRITISH COLUMBIA
CARLETON UNIVERSITY
SIMON FRASER UNIVERSITY
THE UNIVERSITY OF TORONTO
THE UNIVERSITY OF VICTORIA

ASSOCIATE MEMBERS:

THE UNIVERSITY OF GUELPH
THE UNIVERSITY OF MANITOBA
McMASTER UNIVERSITY
L'UNIVERSITÉ DE MONTRÉAL
QUEEN'S UNIVERSITY
THE UNIVERSITY OF REGINA
SAINT MARY'S UNIVERSITY

UNDER A CONTRIBUTION FROM THE
NATIONAL RESEARCH COUNCIL OF CANADA

OCTOBER 2005

The contributions on individual experiments in this report are outlines intended to demonstrate the extent of scientific activity at TRIUMF during the past year. The outlines are not publications and often contain preliminary results not intended, or not yet ready, for publication. Material from these reports should not be reproduced or quoted without permission from the authors.

Experiment 715
Weak interaction symmetries in β^+ decay of optically trapped ^{37,38m}K

(J.A. Behr, M.R. Pearson, TRIUMF; K.P. Jackson, TRIUMF/SFU)

We update our progress in testing the standard model using optically trapped ^{38m}K and ^{37}K. The pure Fermi β^+ decay of ^{38m}K is a sensitive probe of scalar contributions to the weak interaction, while the decay of polarized ^{37}K can be used to search for right-handed currents and time-reversal symmetry violating interactions. The background and experimental set-ups for these experiments have been described elsewhere (Expt. 715, TRIUMF 2002 Annual Report), so we provide here only a brief report on recent progress. Our tensor interaction experiment, Expt. 956, is described elsewhere in this Annual Report.

Scalar search status

Our result for the β-ν correlation parameter $\tilde{a}$= $0.9981 \pm 0.0030^{+0.0032}_{-0.0037}$ is an improvement over previous results in the literature. It is therefore the best limit on general scalar interactions coupling to the first generation. It is now in press [Gorelov *et al.*, Phys. Rev. Lett. (in press)].

Scalar interactions can generally be divided into those that couple only to standard model left-handed νs and those that couple to right-handed νs. Recent theoretical progress has pointed out that indirect limits from the pseudoscalar decay $\pi \rightarrow e\nu$ constrain most of the parameter space at a better level than our experiment, but scalars coupling to particular combinations of left- and right-handed νs are left unconstrained [Campbell and Maybury, Nucl. Phys. B (in press)].

We usually place this in the context of other physics by quoting a sensitivity to scalars with mass to coupling ratios compared to the ratio of the W mass to the electroweak coupling. This requires a form factor g_S relating the quark-lepton scalar interaction to the nucleon- and nucleus-lepton interactions, defined by the equation $\langle p|\bar{u}d|n\rangle = g_S(q^2)\bar{u}_p u_n$. Although there are now lattice gauge calculations for this quantity at zero momentum transfer, to compare such numbers to particle searches can require this form factor as a function of momentum transfer. The scaling is thought to be well-understood [Pospelov, private communication], but the details are best left up to constraints on particular models of particular particle interactions, rather than attempting to cite general limits.

Future: extraction of Fierz interference term The present publication was for data with $E_\beta > 2.5$ MeV, half the Q-value. Experimentally, this avoids a number of complications, including backscattered βs and singles backgrounds in the β detector from the 2.17 MeV γ-ray from decay of the ^{38}K ground state.

There is great value in extending the experiment to lower E_β, because the Fierz interference term b depends on m/E_β. This term is linearly dependent on scalar interactions that couple to left-handed νs, so isolating it from $\tilde{a}$ is useful. The limits from the Q-dependence of the superallowed ft values are very stringent, but these do require isospin mixing corrections to be relatively correct across different major shells, a stricter requirement than needed for V_{ud}. So it is worthwhile to search for this effect within one experiment. Based on an analysis of the TOF spectra, our statistical error on b in the present data set is about four times the recent limits of Towner and Hardy. Systematic error analysis is proceeding, along with an extension of the angular distribution reconstruction to lower energies as a systematic check.

ISAC is now producing five times as much ^{38m}K as when we took this data. A larger MCP would gather a higher fraction of β-Ar^{+1} recoils (currently 89% for $T_\beta > 2.58$ MeV), which would reduce one source of several systematic errors. We are considering whether an upgrade of the experiment might be worth pursuing.

Polarized measurements

Our result for the neutrino asymmetry in the decay of polarized ^{37}K is $B_\nu = -0.771 \pm 0.020 \pm 0.011$, consistent with the standard model prediction $B_\nu = -0.7692$. The largest error is from knowledge of the displacement of the trap position for the two different polarizations. We could measure this better in the future by taking more snapshots of the cloud expansion with the MOT light.

This is the only measurement of a ν asymmetry other than in neutron decay, and has achieved similar accuracy. This constrains a W_R boson coupling to right-handed νs to have mass >170 GeV/c^2 (90% confidence), a result which is not yet competitive with the world average of other β-decay experiments. D. Melconian is completing his SFU Ph.D. and a publication on this topic.

Data were taken under a variety of exploratory experimental conditions, and about 2/3 of the data set was compromised by a combination of poor overlap of the optical pumping beam with the cold atom cloud and imperfect alignment of the magnetic field with the optical pumping axis. We are working experimentally to correct these deficiencies. The present method used (switching off the MOT and optically pumping the atoms on millisecond timescales) can be projected to produce better than 0.5% errors if we pursue it with

modest upgrades. It would be preferable to do these experiments in a trap environment, and we describe these efforts in the next section.

CFORT We are working to develop a circularly-polarized far-off resonance trap (CFORT) which promises extremely high polarizations because only the $M_F = F$ state is trapped and all others are repelled. It is expected that we can achieve >99.9% polarization. This type of trap was developed and loaded efficiently with Rb atoms by JILA [Miller *et al.*, Phys. Rev. **A66**, 023406 (2002)].

As a first step, we have recently succeeded in loading ^{39}K atoms into a far off-resonance dipole force trap (FORT) using linearly polarized light. We have loaded ≈4% of the MOT atoms into the FORT, and achieved FORT lifetimes between 1 and 2 s. This is the M.Sc. thesis data of E. Prime. Work is progressing to improve the loading efficiency and to cool the atoms within the FORT. Light for the MOT for this set-up comes from the 899-21 ring (the MOPA chip has died). The MOT light must be carefully tuned in frequency and power to minimize the temperature of the atoms in order to successfully load the FORT. The FORT uses 700 mW of light from the MBR-110 ring, after first order diffraction in an acousto-optic modulator.

We show the FORT lifetime as a function of detuning from resonance in Fig. 41. The lifetimes are consistent with expected heating from real absorption of photons near the resonance. At larger detunings, another effect is dominating that is not understood. This could be some combination of heating from pointing effects, power, and frequency instability of the FORT laser, or resonant photoassisted dimer formation. Note that the trap has very short lifetimes and trapping efficiency in between the D1 and D2 resonances.

The eventual goal is to use circularly polarized light for the FORT. An intermediate goal would be to optically pump within the FORT environment to polarize the atoms, to produce a better-controlled polarized cloud localization.

MBR-110 upgrade The commercial upgrade to the fully frequency-locked system is incomplete, due to unreliable commercial electronics and etalon hardware and poor support from the company. In the 899-21, the lock to the ring mode is maintained by one ("thick") etalon with 10 GHz free spectral range, and the mode of that etalon is selected by a 200 GHz ("thin") etalon. In the MBR both functions are combined in a single 200 GHz etalon with narrow finesse. This is a very finicky system, and after a great deal of struggle with hardware and electronics, the lock to one cavity mode is made difficult for potassium because it lies close to an oxygen molecular resonance. Complete nitrogen purging of the laser cavity is necessary to obtain an etalon lock (in the 899-21 this merely decreases the power, and the lock is robust over an order of magnitude of output power). It is possible this will be satisfactorily resolved soon.

Potassium $5P_{1/2}$ lifetime We have measured the natural decay lifetime of the $5P_{1/2}$ state in potassium by pulsed excitation using our 405 nm narrow diode laser, followed by non-resonant photoionization to monitor the state population. The result for the lifetime is $\tau = 137.6 \pm 1.3$ ns, an improvement compared to previous results in the literature. If we were to measure the $5P_{3/2}$ lifetime with similar accuracy, a detailed comparison and test of the oscillator strength anomaly could be made, and this is one small test of detailed many-body calculations in alkali atoms of use for atomic parity violation. In reality, we pursued this as a test of experimental methods to be used in francium. Our probe of the excited-state population using non-resonant photoionization has a number of problems, including subtle coherent effects induced by this active probe, and we do not intend to use this method in the future. A paper on the lifetime has been submitted.

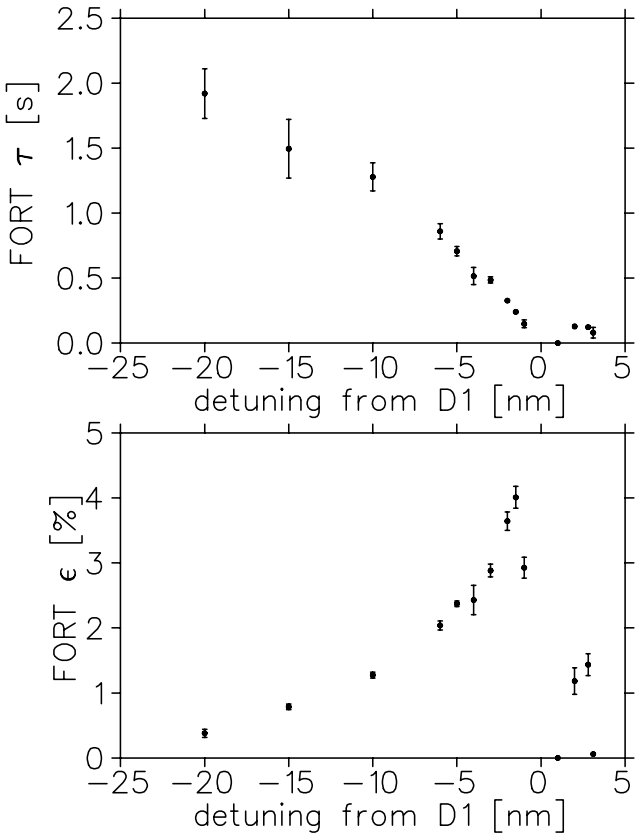

Fig. 41. FORT lifetime τ and loading efficiency ϵ as a function of detuning from the D1 resonance.

Experiment 823
Pure Fermi decay in medium mass nuclei
(G.C. Ball, TRIUMF)

Precise measurements of the intensities for superallowed Fermi $0^+ \rightarrow 0^+$ β decays have provided a demanding test of the CVC hypothesis at the level of 3×10^{-4} and also led to a result in disagreement with unitarity (at the 98% confidence level) for the CKM matrix. Since this would have profound implications for the minimal standard model, it is essential to address possible "trivial" explanations for this apparent non-unitarity, such as uncertainties in the theoretical isospin symmetry-breaking correction. Uncertainties in the calculated Coulomb corrections can be studied by extending the precision β-decay measurements to heavier ($A \geq 62,\ T_z = 0$) odd-odd nuclei where these corrections are predicted to be much larger [Towner and Hardy, Phys. Rev. **C66**, 035501 (2002)]. The primary goal of the Expt. 823 experimental program is to measure the half-lives and branching ratios for the superallowed β-decay of these radioactive nuclei produced at ISAC. The early measurements focused on ^{74}Rb (see TRIUMF 1999–2002 Annual Reports).

High precision decay measurements of the superallowed β-emitter ^{62}Ga

A preliminary measurement of the half-life of ^{62}Ga, the first in the series of ($A \geq 62,\ T_z = 0$) odd-odd superallowed β-emitters was carried out in the spring of 2003. The long-lived (9.74 m) isobar ^{62}Cu was a significant contaminant that limited the precision of this measurement. A preliminary analysis of these data was reported previously (see TRIUMF 2003 Annual Report). The final result, 116.01 ± 0.19 ms, is statistically consistent with all previous measurements [Canchel *et al.*, Eur. Phys. J. (in press)] and references therein]; and the world average is 116.17 ± 0.04 ms. Approval has been obtained to substantially improve the precision of the present measurement to the required precision of 0.05% once the TRIUMF resonant ionization laser ion source (TRILIS) is fully operational.

Non-analogue Fermi and Gamow-Teller branches in the superallowed β-decay of ^{62}Ga have been investigated recently at ISAC using the 8π spectrometer. Since the Q_{EC} value for this decay is large, there are a large number of excited 1^+ states in the daughter nucleus predicted to be populated through GT transitions. These transitions, together with non-analogue Fermi (F) branches must be taken into account to determine the partial half-life of the superallowed transition. However, their individual intensities are very small and many of them cannot be detected with high-resolution gamma spectroscopy. In a previous study [Piechaczek *et al.*, Phys. Rev. **C67**, 051305(R) (2003)] of the superallowed β-emitter ^{74}Rb we have shown that this problem can be overcome with the help of theory. It is not necessary to reconstruct the GT strength function of the decay, only the total amount of non-superallowed feeding must be determined. The low-lying levels in ^{62}Zn act as collector states for a large fraction of the non-superallowed feeding and by observing their de-excitation, the larger part of their feeding can be determined. The remaining component, which directly feeds the ^{62}Zn ground state, can be estimated from shell-model calculations provided they reproduce well the relative feeding to excited levels in ^{62}Zn. In previous studies of the β-decay of ^{62}Ga [Hyman *et al.*, Phys. Rev. **C68**, 015501 (2003)] it was only possible to observe the γ-decay of the first excited 2^+ level in ^{62}Zn.

A beam of $\sim$1600 ^{62}Ga ions/s was produced during the first beam development run with TRILIS (see ISAC Ion Source Development, TRIUMF 2003–2004 Annual Reports for details). A production target of 24 g/cm^2 ZrC was bombarded with 500 MeV protons at an intensity of 35 μA. TRILIS used an ionization scheme that required frequency tripling of the titanium sapphire laser light. Although the laser-ionized ^{62}Ga beam intensity was only increased by a factor of two over that obtained with a surface source in the previous high-precision lifetime measurement, the isobaric contaminant ^{62}Cu was reduced by a factor of $\sim$20. The activity was implanted into the 8π collector tape that was moved every 14 s to prevent the build-up of longer-lived contaminants. The β particles were detected by the SCEPTAR array and recorded cycle by cycle using multichannel scalers. In addition, prescaled β singles, and $\beta - \gamma$ coincidence events were recorded event by event. Portions of the coincident γ-ray spectra obtained when the beam was on and one second after the beam was turned off, but before the tape was moved, are shown in Fig. 42. The peaks observed at 851 and 954 keV correspond to the decay of the first and second 2^+ levels in ^{62}Zn, respectively. The γ-ray at 1387 keV is attributed to the $0_2^+ \rightarrow 2_1^+$ transition. From a preliminary analysis of these data it was possible to observe the decay of the lowest five known 2^+ levels in addition to the feeding of several 1^+ levels up to $\sim$5–6 MeV excitation in ^{62}Zn. As a result, from these data it should be possible to determine the superallowed branching ratio with the required precision of $<$0.1%.

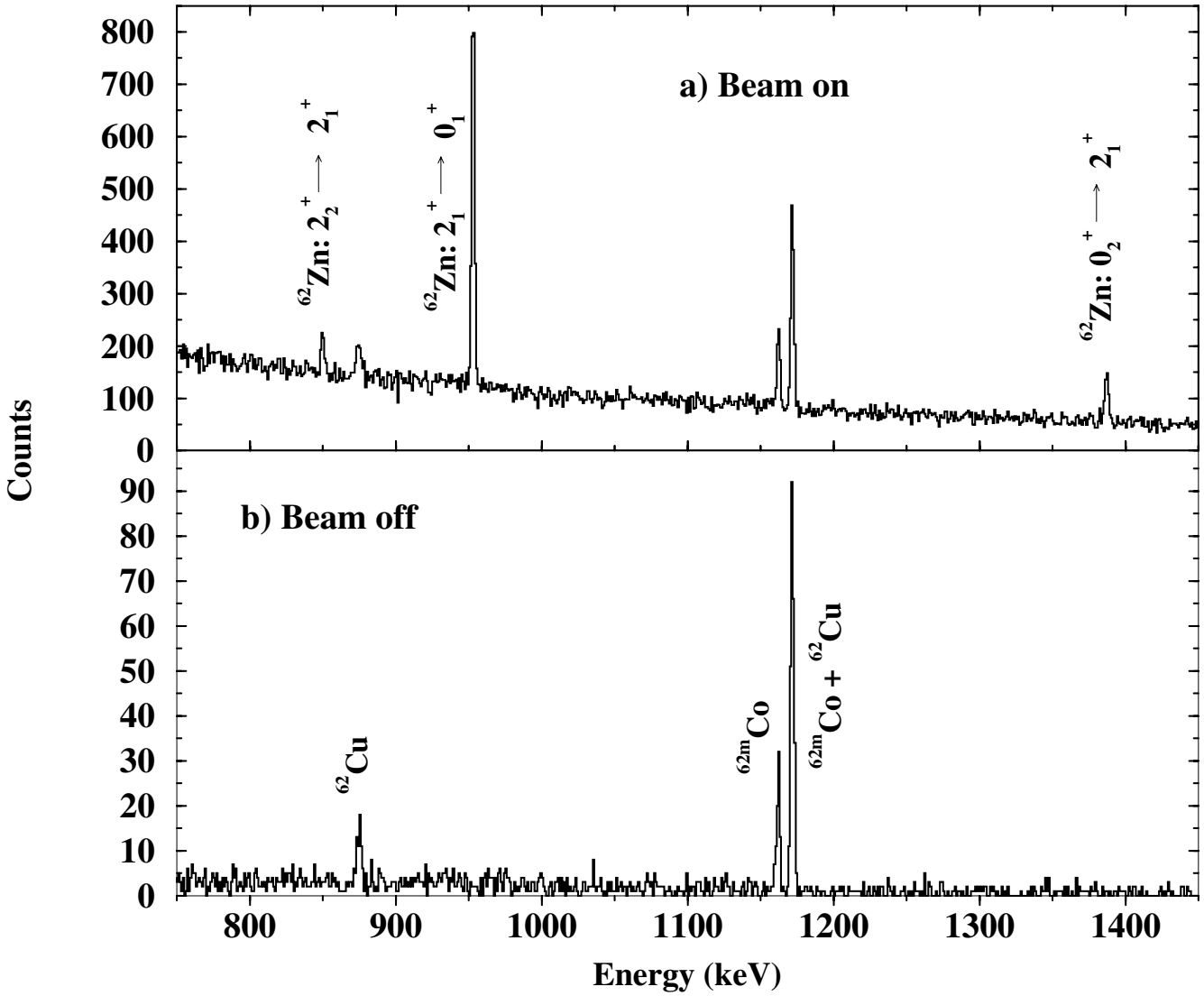

Fig. 42. Portions of the coincident γ-ray spectra obtained in the β-decay of ^{62}Ga: a) during the time in the cycle when the beam was on and b) one second after the beam was turned off. Known transitions in ^{62}Zn as well as peaks resulting from the decay of long-lived isobaric contaminants in the mass 62 beam are identified.

Experiment 893
The hyperfine field of rubidium in iron
(P.P.J. Delheij, TRIUMF)

Introduction

The goal of this experiment is the measurement of the hyperfine field for dilute Rb implanted in Fe. The latest theoretical calculations for the elements from Rb to Xe were able to reproduce the experimental values at the few per cent level [Cottenier and Haas, Phys. Rev. **B62**, 461 (2000)]. The only exception is Rb for which a discrepancy of a factor –5 exists. The NMRON (nuclear magnetic resonance with oriented nuclei) technique can deliver reliable experimental values for the hyperfine field with errors at the 10^{-3} level or better. A beam of ^{79}Rb, the most suitable isotope for this measurement, can be produced at TRIUMF-ISAC with sufficient intensity. Leading up to a measurement with Rb, considerable effort was spent on NMRON development. Test measurements with ^{57}Co and ^{60}Co followed. In view of the beam schedule, an exploratory experiment with ^{22}Na was brought forward and encouraged by the EEC. With this measurement a new mass region was entered for NMRON, being the first one below the element manganese. In addition a new technique was developed by applying NMRON in zero external magnetic field. This avoids the uncertainty from the extrapolation if the zero field resonance frequency must be derived from the field dependence of measurements in non-zero fields. Another new development was the observation of the beta asymmetry through the mea-

surement of the positron annihilation gammas. This provides, independently, the sign of the hyperfine interaction. In such a situation, the simultaneous relaxation of the polarization and the alignment in the sample can be compared.

For these measurements the geometry consisted of a 0.25 mm thick and 10 mm diameter sample disk in the horizontal plane, soldered with Wood's metal on the vertical cold finger that is attached to the dilution refrigerator. A magnetic field up to 1.5 T can be applied horizontally in the east-west direction. So, the cold finger reaches the centre of the magnet through the split. HP-Ge detectors were located east, west and north at a distance of 100 mm from the centre of the sample. A two loop NMR coil with a diameter of 20 mm and a separation of 20 mm between the loops (the axis of the loops is aligned along the north-south direction) produced the rf field for the NMRON measurements.

NMRON development

At the start of 2004 there were indications that the NMRON efficiency at 300 MHz was a factor 10 lower than the 50% we had measured several times for ^{60}CoFe at 166 MHz. A mockup of our NMR probe assembly showed 1) a rather small variation of the signal from the pickup loop as a function of the relative orientation of the transmitter coil and the pickup loop, and 2) a poor agreement of the frequency dependence of the observed and the calculated impedance. Then, it was suggested to remove the pickup loop and split the damping resistance, which is mounted in series with the transmitter coil, in such a way that it would include a 50 Ω resistor. The voltage drop over this resistor was brought out of the cryostat as a measure of the rf current in the transmitter coil and consequently the rf magnetic field amplitude.

Tests with Co sources

After implementing the new NMR arrangement, it was tested with new sources of ^{57}CoFe at 295 MHz and ^{57}CoNi at 123 MHz.

Thereafter, the cold beam line was connected to the cryostat. The test with ^{57}CoFe was repeated and our old ^{60}CoFe was measured. The purpose of these tests was to demonstrate the performance of the LTNO system at ISAC by reproducing previously measured parameters like the resonance frequency and especially the NMRON efficiency. For these long lived sources NMRON efficiencies varied from 50% to 70%. By increasing the rf amplitude the off-resonance anisotropy decreased but the destroyed fraction increased. This can be explained by the larger amplitude depolarizing the nuclei near the surface on-resonance as well as off-resonance. At the same time the larger rf amplitude reaches further into the sample destroying on-resonance a larger fraction of the Co orientation. It implies that the diffusion depth of our thick samples is limited to about 1 μm, the penetration depth of the rf field at these frequencies. This was accomplished by a short diffusion time when the samples spend only approximately 5 min on the temperature trajectory 600 °C → 800 °C → 600 °C.

Furthermore, the spin-lattice relaxation time was measured for ^{60}CoFe in an external magnetic field of 0.2 T, 0.8 T, and 1.4 T. For ^{57}CoFe it was measured in a field of 0.2 T, 0.4 T and 0.6 T. The data in the lowest field are shown in Figs. 43 and 44. This relaxation time is related to the spin dynamics, which is sensitive to the sample structure. The good agreement with values in the literature gives confidence that the quality of our sample preparation procedure is adequate.

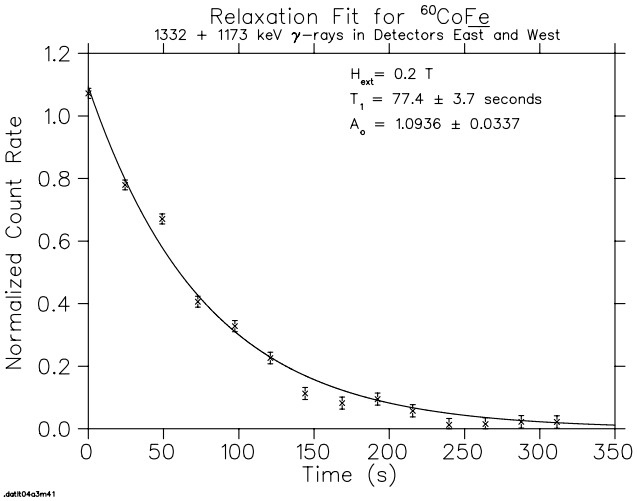

Fig. 43. Relaxation curve of ^{60}CoFe. At time = 0 the frequency modulation of the rf field is turned off.

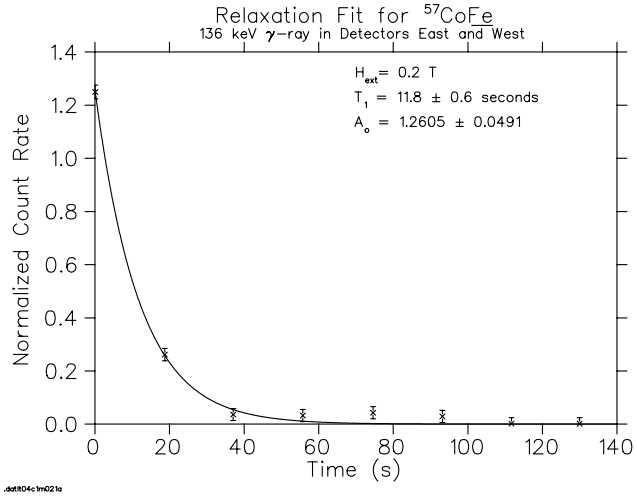

Fig. 44. Relaxation curve of ^{57}CoFe. At time = 0 the frequency modulation of the rf field is turned off.

The experiment with ^{22}Na<u>Fe</u>

At this stage it was considered to explore the low mass region and provide accurate and reliable NMRON data to achieve a comparison with theoretical calculations of the hyperfine field at the same level as in the Rb-Xe region. This is appropriate at ISAC because several astrophysics experiments require beam development efforts near mass 20. In this mass region particularly for dilute oxygen in Fe there exist large discrepancies between the values of the hyperfine field from different experimental techniques. Theoretical calculations give a hyperfine field with the opposite sign, see for example the review in Severijns *et al.* [Hyp. Int. **60**, 889 (1990)]. But no NMRON measurements have been reported previously for impurities with a lower mass than manganese. To explore the feasibility in this mass region an experiment with long-lived ^{22}Na<u>Fe</u> was considered. ^{22}Na, with a lifetime of 2.7 years, is available copiously at the ISAC facility and the required resources to produce a sample are fairly limited. A challenge was the rather low expected anisotropy (the nuclear magnetic moment is +1.746(3) n.m.) of 1% to 2% for the 1274 keV gamma transition. Therefore, we explored with ^{57}Co<u>Fe</u> whether accuracies at the 10^{-3} level could be obtained for the γ-ray peak areas during a NMRON scan. When this turned out favourably, the pilot measurement with ^{22}Na<u>Fe</u> was submitted to the EEC and it received a positive judgement. Subsequently, these measurements were carried out over the summer. One of our standard Fe disks, polished and annealed as usual, was mounted in the ISAC collection station. Then this sample was cooled in the low temperature nuclear orientation set-up at ISAC to a temperature near 8 mK.

In view of the long relaxation time, 16 runs of 15 min duration were taken at each frequency leading to approximately 24 hours for a complete rf scan. At all magnetic fields a scan stepping up in frequency and a scan stepping down in frequency were taken. For each frequency in the plots frequency modulation with a range of $\pm 1/2$, the frequency step size was applied. The modulation consisted of ramping up the frequency with a sawtooth pattern at a repetition rate of 15 Hz. Resonance frequencies were determined in external magnetic fields of 0.2 T, 0.4 T, 0.6 T and 1.4 T. Scans for the lowest and highest magnetic field are plotted in Figs. 45 and 46. These graphs show that, as expected, the intensity change for the 1274 keV γ-ray has the same sign for the detectors along the external magnetic field and the detector perpendicular to the magnetic field shows a resonance amplitude with the opposite sign.

In contrast, for the 511 keV gammas, the east and west detectors, parallel and antiparallel to the magnetic field, show resonance amplitudes with opposite

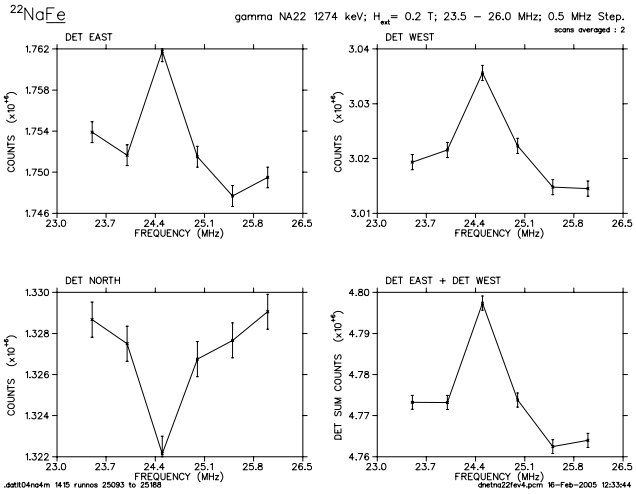

Fig. 45a. NMRON resonance in the anisotropy of the 1274 keV gamma transition with $H_{ext} = -0.2$ T.

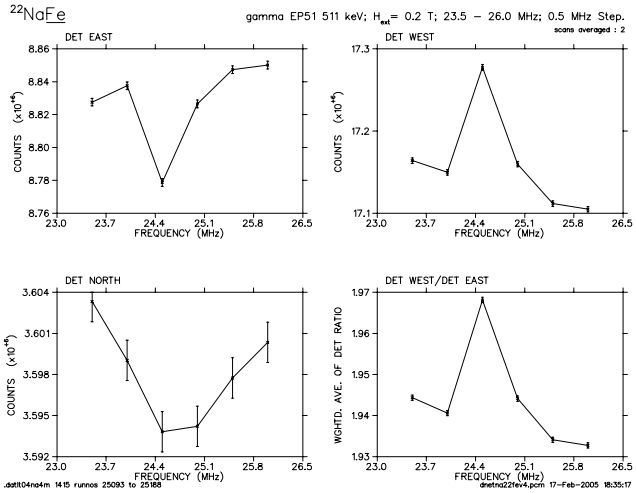

Fig. 45b. NMRON resonance in the asymmetry of the 511 keV gammas, that originate from the annihilation of positrons coming from the beta decay, with $H_{ext} = -0.2$ T.

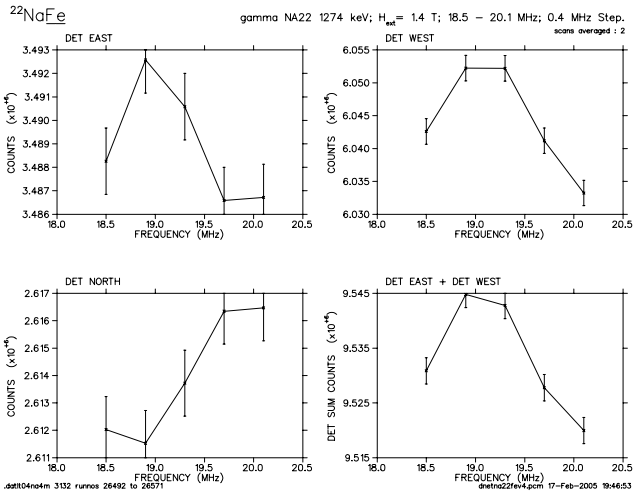

Fig. 46a. NMRON resonance in the anisotropy of the 1274 keV gamma transition with $H_{ext} = -1.4$ T.

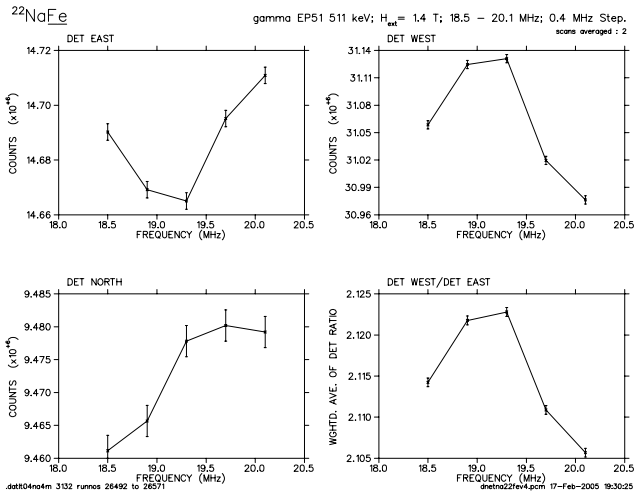

Fig. 46b. NMRON resonance in the asymmetry of the 511 keV gammas, that originate from the annihilation of positrons coming from the beta decay, with $H_{ext} = -1.4$ T.

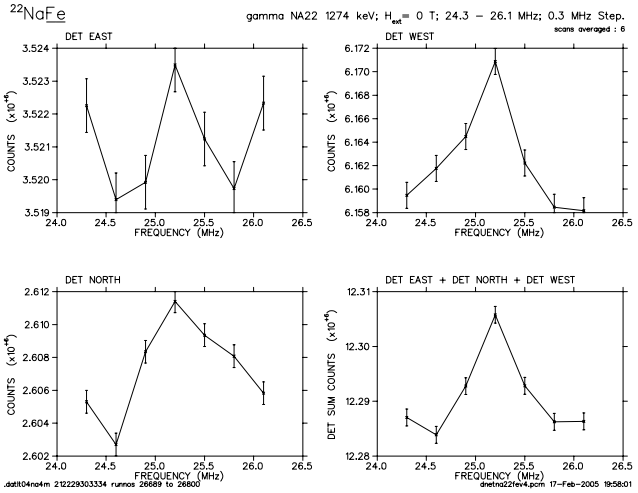

Fig. 47. NMRON resonance in the anisotropy of the 1274 keV gamma transition without an external magnetic field, $H_{ext} = 0$ T.

sign. For the north detector, perpendicular to the magnetic field, the amplitude is an order of magnitude smaller. This can be understood if it is realized that the positrons, which are emitted asymmetrically from this polarized sample, meet only a substantial material mass at the cryostat wall. Therefore, the cryostat wall in front of the Ge detectors serves as a converter of positrons propagating towards a particular detector. As a consequence the rate of the 511 keV gammas reflects the positron asymmetry. To our knowledge this effect has never been applied in LTNO or NMRON experiments. A lowering of the resonance frequency versus increasing external magnetic field implies a negative sign for the hyperfine interaction. The data at 1.4 T show a negative frequency shift which also determines the negative sign for the hyperfine field. It should be noted that the width is approximately a factor 1.5 larger and the amplitude a factor 2 smaller in comparison with the resonance data at 0.2 T. These factors were considerably smaller than could be expected for this ratio of 7 in the external magnetic fields.

The direction of our external magnetic field was calibrated against the magnetic field of the TRIUMF main cyclotron. This provides, through the positron asymmetry, an independent measurement of the sign of the hyperfine interaction for Na<u>Fe</u>.

NMRON scans were also taken without an external magnetic field applied to the sample as is shown in Fig. 47. We have observed in the past that, without an external magnetic field, the nuclear spins are confined to the plane of the Fe disk. This provides an oriented nuclear spin ensemble with a rather uncommon character. There is no axial symmetry. With this nuclear orientation it was neverthelesss possible to observe an NMRON resonance. In this geometry all three Ge detectors occupy equivalent positions for the angular distribution.

In this way the hyperfine field can be determined without errors from an extrapolation versus the magnetic field requiring an estimate of the external field that saturates the magnetization and also the estimate of the demagnetizing factor. Our data gave a resonance frequency of 25.200 ± 0.013 MHz. With a magnetic moment of 1.746 ± 0.003 n.m., this leads to a measured magnetic field of -5.67 ± 0.01 T where the size of the error is determined by the uncertainty in the magnetic moment. After applying the correction for the Lorentz field, which is $1/3 \times$ the saturation magnetization in Fe (which is 2.196 T) under the assumption of a spherical cavity for the impurity atom, the result is a value of 6.40 ± 0.01 T. This value is consistent with the result -5.8 ± 0.5 from a previous integral LTNO experiment with ^{24}Na [Vanderpoorten *et al.*, Hyp. Int. **75**, 331 (1992)] which had a considerably larger uncertainty. Furthermore, the relaxation time was determined in an external field of 0.2 T as shown in Fig. 48a for the gammas and Fig. 48b for the positrons. Within the errors there is no significant difference in relaxation times of the dipolar nuclear orientation component (positrons) and quadrupolar orientation component (gammas).

The experiment with ^{79}Rb<u>Fe</u> and ^{79}Kr<u>Fe</u>

In the fall, NMRON was attempted with ^{79}Rb<u>F</u>e. The anisotropy for the intensity ratio of the 688 keV and 622 keV gamma transitions turned out a factor two smaller than we had observed previously. In this context it was not so surprising that the NMR linewidth was a factor 10 larger than expected and consequently the amplitude, by the same factor, smaller. About 30 hrs of beam time was available to get to the result shown in Fig. 49, leaving no opportunity to confirm

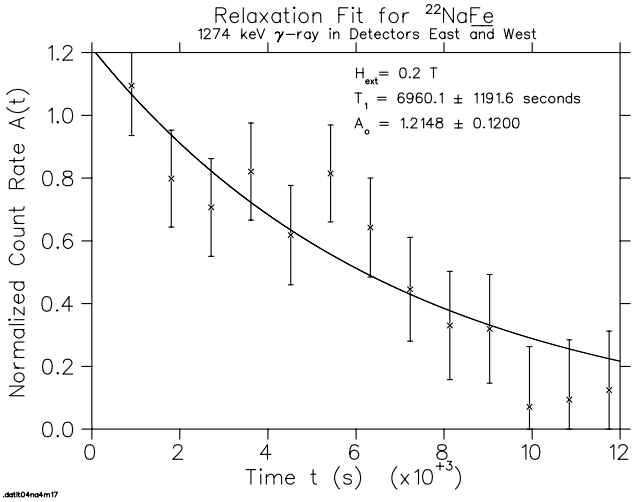

Fig. 48a. Relaxation curve from the 1274 keV transition for ^{22}NaFe. Shown is the normalized rate, averaged for $\mathrm{DET_{east}}$ and $\mathrm{DET_{west}}$. At time = 0 the frequency modulation of the rf field is turned off.

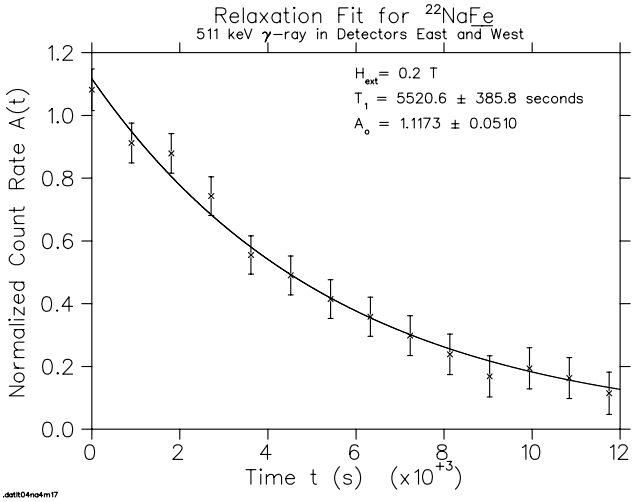

Fig. 48b. Relaxation curve from the annihilation gammas for ^{22}NaFe. Shown is the normalized ratio of $\mathrm{DET_{west}/DET_{east}}$. At time = 0 the frequency modulation of the rf field is turned off.

it with a different external field. In view of the reduced integral anisotropy (while the temperature was certainly not worse than previously) a reasonable conclusion was that the sample surface had been damaged in the last stages of the mounting procedure.

Plans were made for a procedure such that the surface could be inspected with XPS and/or auger electron spectroscopy to prevent a repeat of this ocurrence.

After the ^{79}Rb had decayed, the intensity of the 511 keV gamma from the positron decay of ^{79}Kr was measured. The intensity was sufficient to observe the asymmetry on cooldown but too low to obtain NMRON results. The results are listed in Table X for two measurements with a magnetic field of –0.2 T

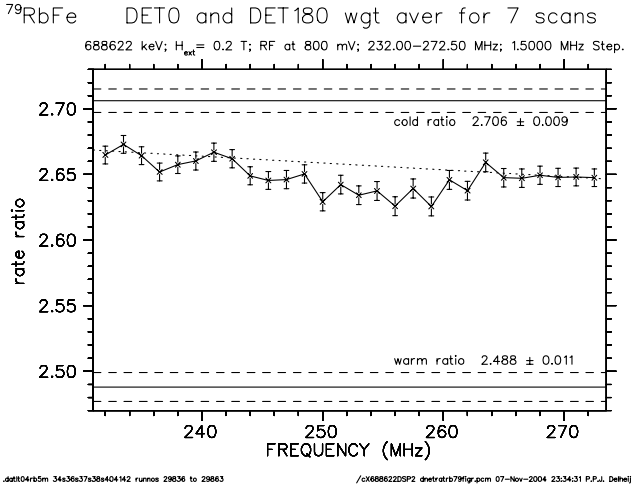

Fig. 49. The measured intensity ratio for the 688 keV and 622 keV transitions is shown versus rf frequency. The dotted line is a least squares fit to the data points at the three highest and three lowest frequencies. Also the cold and warm ratio without rf field are shown.

Table X. Change of the positron decay asymmetry on cool down of the sample for two values of the external magnetic field.

H_{ext}	Warm	Cold	Delta
–0.2 T	2.548(7)	2.504(7)	+0.044(10)
+0.8 T	3.243(14)	3.319(14)	–0.078(20)

and +0.8 T. The first field was the same as used for the measurement on ^{22}Na that is shown in Fig. 45. Since the sign of the magnetic moment (+1.124(10)) is the same too, it is straightforward to derive that the sign of the hyperfine field for ^{79}KrFe is negative confirming the result from a previous measurement [Severijns *et al.*, Hyp. Int. **43**, 415 (1988)].

Summary

With ^{22}NaFe a beam implanted sample was produced that extended the mass range and frequency range for NMRON considerably. For mass 79, a not yet convincing NMRON result was obtained. The observation of NMRON without an external magnetic field and the measurement of the beta asymmetry through converted positrons were methods (to our knowledge) not applied previously.

Experiment 909
Isospin symmetry breaking in superallowed Fermi β-decays
(G.F Grinyer, Guelph)

Precision measurements of the ft values for superallowed $0^+ \rightarrow 0^+$ Fermi β-decays between isobaric analogue states provide demanding tests of the standard model description of electroweak interactions. To date, superallowed ft values have been determined at the ±0.1% level for nine nuclei between ^{10}C and

^{54}Co. Once corrected for small radiative and isospin symmetry-breaking effects, their consistency has confirmed the conserved vector current (CVC) hypothesis at the level of 3×10^{-4}. From these studies, the Cabibbo-Kobayashi-Maskawa (CKM) matrix element, V_{ud}, can be derived by comparing the β-decay data with pure leptonic muon decay. Combining the results from superallowed Fermi beta decay studies with the present knowledge of V_{us} and V_{ub}, indicates a violation of CKM unitarity at the 98% confidence level [Towner and Hardy, Phys. Rev. **C66**, 035501 (2002)]. Although recent measurements indicate the accepted value of V_{us} may be the cause of this discrepancy, these results are still under intense scrutiny and must be confirmed by independent measurements.

Should this discrepancy be firmly established, it would indicate the need for new physics, either in terms of explicit quark effects in nuclear structure or an extension of the minimal electroweak standard model. Before a definitive conclusion can be reached, all uncertainties contributing to the unitarity test must be carefully scrutinized and, if possible, reduced. For V_{ud}, the dominant uncertainties are those associated with theoretical corrections to the ft values, and the search for systematic effects has focused on the nuclear-structure dependent δ_C corrections that account for the breaking of isospin symmetry by charge-dependent forces in the nucleus.

Experiment 909 involves a series of measurements with the 8π spectrometer and the scintillating electron positron tagging array (SCEPTAR) aimed at constraining the above-mentioned isospin symmetry-breaking corrections in superallowed Fermi β-decays. This program will take advantage of the unique beams of radioactive ions available at ISAC to study particular decays in which the predicted δ_C corrections show the greatest model sensitivity. An initial focus of Expt. 909 will be on lifetime and branching ratio measurements for ^{34}Ar, with the aim of establishing the superallowed ft value at the $\pm 0.1\%$ level. The first objective will be to improve the current half-life precision by approximately one order of magnitude. These measurements will be carried out by collecting samples of ^{34}Ar at the centre of the 8π and following their decay for $\sim$30 half-lives by time-stamping γ-rays emitted from excited states in the daughter ^{34}Cl populated in Gamow-Teller decay branches of ^{34}Ar.

In anticipation of ^{34}Ar beams from the ISAC ECR ion source in spring, 2005, tests of the experimental techniques to be employed in Expt. 909 were carried out with radioactive ^{26}Na beams. This isotope was chosen because: i) high yields were available from ISAC surface ion sources, ii) the half-life ($\sim$1.07 s) is similar to ^{34}Ar, iii) the daughter ^{26}Mg is stable, and iv) $\sim$99% of ^{26}Na β-decays are followed by an 1809 keV γ-ray transition in ^{26}Mg, facilitating tests of the γ-ray lifetime technique to be employed for ^{34}Ar. The first requirement was to determine a precise value for the ^{26}Na lifetime. To this end, a ^{26}Na beam was delivered in 2002 to the fast tape system at the ISAC general purpose station (GPS) and its lifetime determined to high precision by the well-established β counting technique with a 4π gas proportional counter. The analysis of these data (a sample of which is shown in Fig. 50) is now complete, and the ^{26}Na half-life has been established as $T_{1/2} = 1.07128 \pm 0.00013 \pm 0.00021$ s, where the first error is statistical and the second systematic.

The second requirement for measurements of precision partial lifetimes is the beta branching ratios to the excited states in the daughter nucleus. In August, 2002, a beam of ^{26}Na at $\sim 10^5$ s^{-1} was delivered to the 8π from a Ta target coupled to a surface ionization source. From the data obtained, a total of 84 γ-rays from 20 excited states in ^{26}Mg were identified (see Fig. 51) with energies between 240 keV and 7.370 MeV and intensities ranging from 0.99 to below 10^{-5} per β-decay. This extends previous work in which 20 γ-rays from 11 populated levels were identified. Combining the precision lifetime measurement from the beta counter at GPS, with the beta branching ratios from the 8π γ-ray spectrometer, and the previously known Q-value allowed a calculation of the ft values for each of 20 excited states in ^{26}Mg. These data in addition to the precision lifetime measurement are reported in a recent publication [Grinyer *et al.*, Phys. Rev. C (in press)].

In April, a beam of ^{26}Na was delivered to the 8π spectrometer to test the methodology and techniques for a γ-ray lifetime measurement of ^{26}Na which will

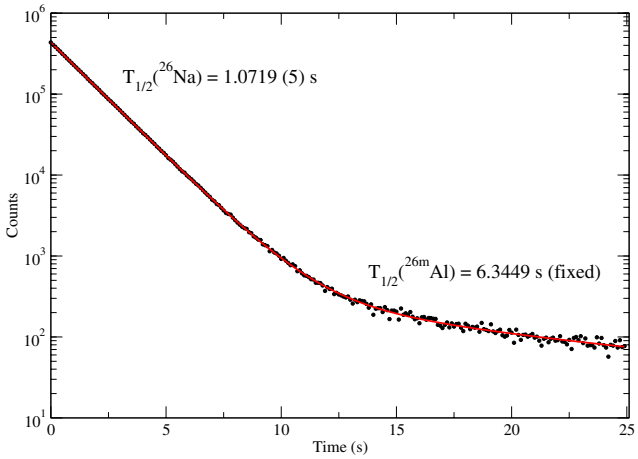

Fig. 50. Decay curve from a single run of β counting ^{26}Na samples with the 4π gas proportional counter at the ISAC GPS. The second (longer lived) decay component results from a small ^{26m}Al contamination of the beam. A total of 24 runs of similar precision were obtained which yielded an overall statistical precision of $\pm 0.03\%$.

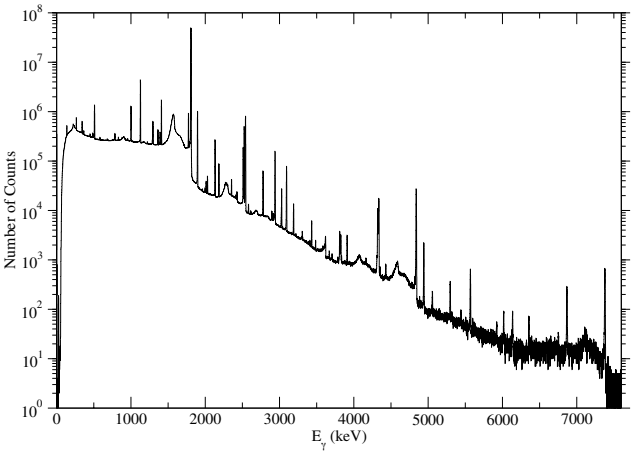

Fig. 51. γ-ray singles spectrum from ^{26}Na decay recorded with the 8π spectrometer at ISAC. In this experiment, the 8π spectrometer was sensitive to beta branching ratios of 2×10^{-5}.

later be employed for ^{34}Ar. These data are currently being analyzed for a comparison with the precise ^{26}Na half-life result determined through β counting. This comparison will provide fundamental insight into systematic effects such as detector pile-up corrections that have not allowed previous γ-ray lifetime measurements to achieve the level of precision ($\sim$0.05%) necessary for distinguishing between the model dependencies of the isospin symmetry breaking corrections described above.

Another key detector that will be employed for the measurements described is SCEPTAR, an array of 20 plastic scintillators which is situated at the centre of the 8π spectrometer. A commissioning run for SCEPTAR using a beam of ^{26}Na took place in June, 2003. Although SCEPTAR will not be essential in the ^{34}Ar lifetime measurement, β–γ coincidences will provide a crucial normalization necessary to perform the ^{34}Ar superallowed β branching ratio determination. In another experimental program (Expt. 985 led by M.B. Smith) which aimed to measure the lifetime and superallowed β branching ratio in ^{18}Ne, SCEPTAR provided an invaluable tool in the identification of small beam contamination components of ^{18}F and ^{17}F during a June, 2004 experiment.

Following measurement of the ^{34}Ar lifetime and branching ratio, subsequent measurements with the 8π and SCEPTAR will focus on an improved determination of these quantities in several other superallowed nuclei. Large, and model-dependent, isospin symmetry-breaking corrections are also predicted for the $A \geq 62$ odd-odd $N = Z$ nuclei. A program of precision lifetime measurements (Expts. 823 and 1028) for these nuclei with the 4π gas proportional counter at GPS is being led by G.C. Ball of TRIUMF. Future experiments with the 8π spectrometer and SCEPTAR will provide branching ratio measurements for these short-lived isotopes. Weak non-analogue Fermi decay branches that provide direct and absolute information on one component of the isospin symmetry breaking will also be measured. The first such measurement with the 8π was performed in December with a beam of $\sim$1600 s^{-1}, ^{62}Ga delivered by the TRIUMF resonant ionization laser ion source (TRILIS). Several γ-ray transitions following weak Gamow-Teller and non-analogue Fermi branches were identified. These data should allow for a determination of the superallowed branching ratio at the <0.1% level. With the continuing development of ion source technology at ISAC, these superallowed and non-analogue Fermi β-decay branching ratio studies will be extended to include ^{26m}Al, ^{38m}K, ^{66}As, ^{70}Br, and ^{74}Rb.

Experiment 921
High-K isomers in the neutron-rich Dy-Hf nuclei
(R.S. Chakrawarthy, TRIUMF; P.M. Walker, Surrey)

The detection and study of high-K isomers is an active area of current nuclear structure research. In particular, one of the goals of a future study involving neutron-rich nuclei in the Dy-Hf region is to search for the possible existence of an "island" of β-decaying high-K isomers. The close proximity of high-K states to the Fermi surface in neutron-rich $A = 170$–190 nuclei makes this region very attractive to search for high-K isomers [Walker and Dracoulis, Hyp. Int. **135**, 83 (2001)]. In two sets of experiments several of the known high-K isomers in the Dy-Hf region, with half-lives ranging from a few ms to several minutes, could be accessed [Smith *et al.*, Nucl. Phys. **A746**, 617 (2004)]. We report here the discovery of a new isomer in the neutron-rich nucleus ^{174}Tm. The $A = 174$ isobaric beam was implanted onto a moveable tape transport facility, with beam-on/beam-off cycling times of 2 s/2 s, 3 s/3 s ("short"), 10 s/10 s and 100 s/50 s. In the short cycling times γ-ray transitions with energies of 100.3 and 152.1 keV were observed, which are known to be present in the ground-state β-decay of ^{174}Er ($t_{1/2}$ = 3.3 min) [Becker *et al.*, Nucl. Phys. **A522**, 557 (1991); Chasteler *et al.*, Z. Phys. **A332**, 239 (1989)].

In the present experiment we found no evidence for the production of ^{174}Er. A new half-life of 2.29(1) s was deduced from γ-time matrices gated by the 100 and 152 keV γ-ray transitions (Fig. 52). A "short" time-gated singles spectrum, obtained by subtracting out the long-lived β decays, shows prominently only the Tm K X-rays and the 100 and 152 keV γ-ray transitions (Fig. 53). Based on the singles and the coincidence data, a new isomer in ^{174}Tm with a half-life

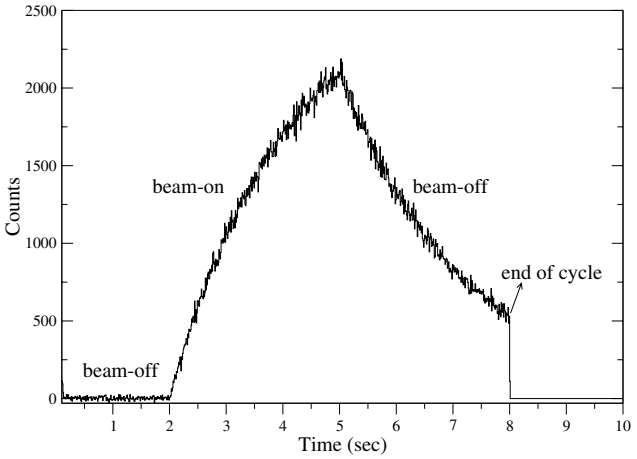

Fig. 52. Time spectrum gated by the 100.3 keV γ-ray transition. The beam-off/beam-on/beam-off tape-cycling times correspond to 2 s–3 s–3 s.

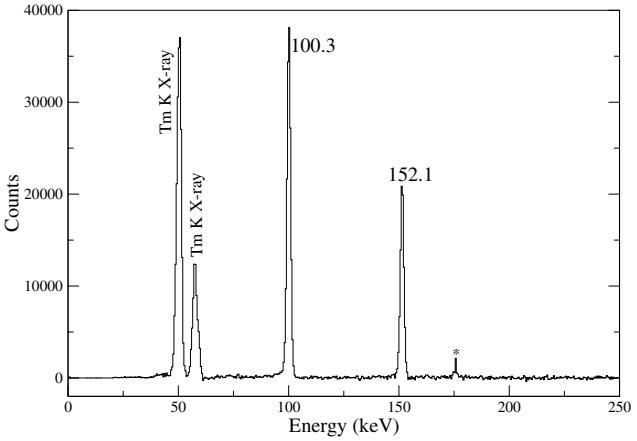

Fig. 53. Singles spectrum in the "short" cycling time of 2 s–3 s–3 s corresponding to the beam-off/beam-on/beam-off periods. The dominant component due to the longer lived ^{174}Tm β-decay ($T_{1/2}$ = 5.4 min) has been subtracted. The peak marked by the asterisk is a remnant of the subtraction procedure.

of 2.29(1) s is established unambiguously. From the coincidence data the K-conversion coefficients for the 100 and 152 keV γ-ray transitions were deduced to be 3.1(1) and 1.13(6) respectively, suggesting mainly M1 multipolarity with an E2 admixture. The new data are in close agreement with the theoretically expected values of 2.69 and 0.82 for M1 multipolarity, respectively, but differ from the values 1.7(3) and 0.54(6), respectively, reported by Becker *et al.* [Nucl. Phys. **A522**, 557 (1991)].

A careful analysis of the singles spectrum (Fig. 53) did not yield any new γ-ray transitions that could be candidate γ-ray transitions between the isomer and the known states. These data suggest the possibility of the existence of very low-energy and highly-converted transitions in the decay of the isomer and the excited states. Furthermore, if the origin of isomerism is presumed to be partly due to K-hindrance (in line with several known examples in this mass region) then this level could possibly have a high K value. Based on systematics and Nilsson model calculations of the single-particle levels in ^{174}Tm, the isomer is tentatively assigned to have a $K^\pi = (8^-)\pi 7/2^-[523]\otimes\nu\, 9/2^+[624]$ Nilsson configuration, while the other excited states may be based on $K^\pi = ((4/5)^+)\pi 1/2^+[411] \otimes \nu\, 9/2^+[624]$ configurations. The levels involved in the isomer decay may have spins greater than the low values suggested from the previous works. The present interpretation would be consistent with the earlier data only if the decay through the 100 and 152 keV transitions originates from a high-spin β-decaying isomer in ^{174}Er instead of the ground-state β-decay of ^{174}Er. The preceeding results have been reported at the ENAM04 conference [Chakrawarthy *et al.*, Proc. ENAM04, Pine Mountain, USA (Eur. Phys. J. A, in press)]. Preparations for an experiment to detect the low energy/highly-converted transitions, using a Si detector-array, are in progress.

Experiment 921 is a collaboration of scientists from TRIUMF, University of Surrey, Colorado School of Mines, Lawrence Livermore National Laboratory, Louisiana State University, McMaster University, Saint Mary's University and University of Guelph.

Experiment 956
Search for tensor interactions in recoil nucleus singles in decay of polarized ^{80}Rb

(J.A. Behr, M.R. Pearson, TRIUMF; K.P. Jackson, TRIUMF/SFU)

Scientific motivation

The recoiling daughter nuclei from the β decay of polarized nuclei have spin asymmetry $A_{\rm recoil} \approx 5/8$ $(A_\beta + B_\nu)$ [Treiman, Phys. Rev. **110**, 448 (1958)], in the limit $Q_\beta >> m_\beta$. This vanishes in the allowed approximation for pure Gamow-Teller decays, making it a very attractive experimental observable because knowledge of the nuclear polarization at 1 to 10% level is sufficient to be competitive. Our novel capability of measuring the recoil nuclei from laser-polarized cold atoms allows this observable to be measured now.

Right-handed currents do not contribute, so $A_{\rm recoil}$ is uniquely sensitive to lepton-nucleon tensor interactions. A renormalizable interaction that Lorentz transforms like a tensor can be generated by the exchange of spin-0 leptoquarks [Herczeg, Prog. in Part. and Nucl. Phys. **46/2**, 413 (2001)].

"Recoil-order" corrections beyond the allowed approximation do produce a nonzero $A_{\rm recoil}$ within the standard model. These produce corrections to the β asymmetry A_β for ^{80}Rb of order 0.01, and we expect similar effects on $A_{\rm recoil}$, so the result will depend on

calculation of the nuclear structure-dependent weak magnetism and first-class induced tensor terms (b and d in Holstein's notation). Our knowledge of these could be tested by measuring the momentum dependence of the recoil asymmetry. We are negotiating for theory support.

The PIBETA collaboration has reported hints of a finite tensor interaction [Frlež, Phys. Rev. Lett. **93**, 181804 (2004)] in $\pi \to \nu e\gamma$ decay, though at a level considerably smaller than that reported at Dubna [Bolotov *et al.*, Phys. Lett. **B243**, 308 (1991)]. Experiment 956 would become competitive with other nuclear β-decay measurements if it achieves 0.01 accuracy in the recoil asymmetry [Herczeg, Phys. Rev. **D49**, 247 (1994)], while $\sim$0.001 level is needed to reach similar sensitivity to the tensor interaction indicated by the π decay experiments. Since the recoil asymmetry vanishes, the degree and knowledge of polarization achieved in Expt. 715 is already sufficient for Expt. 956.

"Resolution" of nucleon form factor question To interpret β decay results in terms of quark-lepton interactions, the form factor $g_T(0)$ defined by: $< p|\bar{u}\sigma_{\mu\lambda}d|n >= g_T(q^2)\bar{u}_p\sigma_{\mu\lambda}u_n$ is needed, and there has been controversy over this quantity [Herczeg, *op. cit.*]. This situation is now in good shape both theoretically and experimentally, because the quantity is related by simple isospin rotation to the "transverse spin" function of the nucleon. This is the last of the nucleon spin functions to be measured, is a source of intense theoretical and experimental (at HERMES) effort, and should be known at the 20% level or better soon [Pospelov, private communication]. This would be more than good enough to allow comparison of a nonzero tensor in nuclear β decay to π decay.

Experiment

In the Expt. 956 apparatus (Fig. 54) the TRINAT β telescope is replaced with a 7.5 × 7.5 cm NaI(Tl) detector. An electric field collects much of the angular distribution from charged recoils into a microchannel plate (MCP). The NaI detector tests the experimental practicality of γ-recoil coincidences. It also serves as a β detector for polarization diagnostics, since β-recoil coincidences in this geometry are proportional to the neutrino asymmetry B_ν. The NaI detects 617 keV γs from the 22% β branch to the first excited 2^+ state of ^{80}Rb. The intent is to measure the "singles" asymmetry for decays to the 2^+ state separately via the γ-ray coincidence. The angular distribution of γ's with respect to the spin direction is given by $W(\theta_\gamma) = 1 - 0.25\ \mathrm{P}_2(\cos\theta)$, so there is no recoil asymmetry induced. That allows measurement of a correction to the total asymmetry to deduce the singles asymmetry for the 1^+ to 0^+ transition, which has

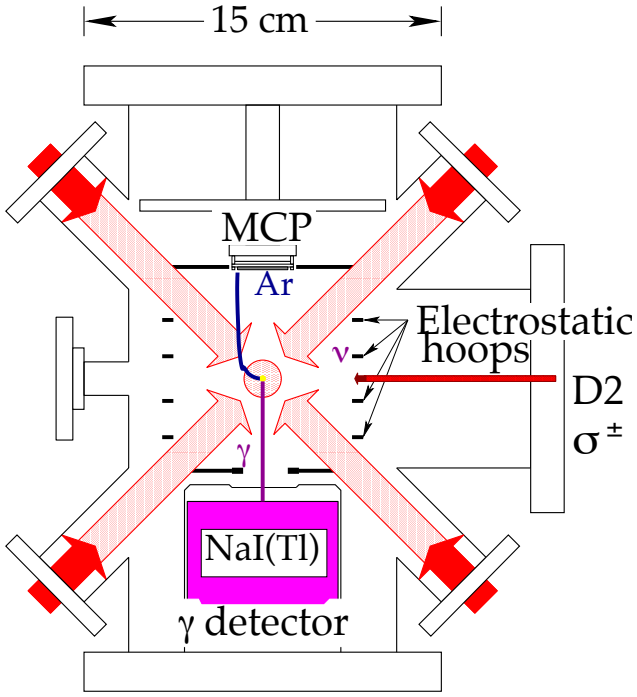

Fig. 54. TRINAT apparatus as modified for Expt. 956. A NaI(Tl) detector for γ-rays replaces the main β^+ telescope. D2 light is used to optically pump ^{80}Rb.

only two recoil-order form factors (b, weak magnestism, and d, induced first-class tensor). That simplifies the nuclear structure corrections needed.

The recoil order effects are expected to enter at $\sim$0.01 level. To reach 0.001 level it will be necessary to measure the momentum-dependence of the recoil asymmetry. This could be done by detecting atomic shakeoff electrons in coincidence with recoils to provide a bias-free TOF trigger.

Another possibility would be a measurement of ^{47}K decay, a much better case for recoil-γ experiments. The β^- decay always produces a measureable charged recoil, increasing count rates and recoil/β ratios by 6× over β^+ decay. The 81% $\frac{1}{2}^+ \to \frac{1}{2}^+$ transition will also only have two form factors, and always produces a γ. A complication will be isospin mixing of this final state with the analogue state, which would produce a nonzero Fermi matrix element and a nonzero A_{recoil} that is constant with recoil momentum. The plan would be to measure both isospin mixing – an interesting observable in its own right – and tensor interaction effects.

Data-taking An ^{80}Rb beam of 6×10^7/s from a Ta target was delivered for several days, enough to make a large start towards the first goal of 0.01 in the integrated singles measurement. This was a thin target optimized for ^{11}Li production. Yields adequate for the final experiment have been produced by 20 μA on 44 g/cm^2 Ta (2×10^9/s) and 40 μA on 22 g/cm^2 Nb

(3×10^{10}/s) in the past, and unpolarized tests were handled by TRINAT data acquisition in 1999 at one hundred times the present count rate. It is also possible to do an experiment in ^{82}Rb, which has similar Gamow-Teller decay branches and ten times greater yields, although the 1.26 minute half-life and the existence of a 6.5 hour isomer will make backgrounds larger.

Nuclear and atomic level diagrams are shown in Fig. 55. The β decay scheme is a relatively simple Gamow-Teller decay. The atom structure has narrow hyperfine splitting, and we trapped it with one 899-21 ring laser. We also use transitions at similar wavelength for the optical pumping.

Our usual atomic physics probe of the polarization is to optically pump with circularly polarized light to the $P_{1/2}$ state. The fluorescence will vanish once the atoms are fully polarized, because the total angular momentum of the initial and final states is the same and the atom no longer absorbs photons. We do not have a 795 nm D1 laser for rb, so for ^{80}Rb we use the $P_{3/2}$ state with the light tuned on resonance for $F = 3/2$ to $F' = 3/2$. Since we pump at about 5 times saturation intensity, there will always be 10–20% of the initial fluorescence by off-resonant excitation of the $F = 3/2$ to $F' = 5/2$ transition.

Signals in nuclear detectors We show in Fig. 56 a NaI spectrum in coincidence with the Kr^{+1} recoils. The low-energy bremsstrahlung tail is reasonably well-correlated with the β^+ direction, providing some on-line diagnostics for polarization with reasonable statistics; however, this will require a full Monte Carlo GEANT simulation to quantify. The 617 keV gamma can be seen as a shoulder on the 511 keV gamma; coincidences with the MCP would let us measure the recoil asymmetry as a function of momentum.

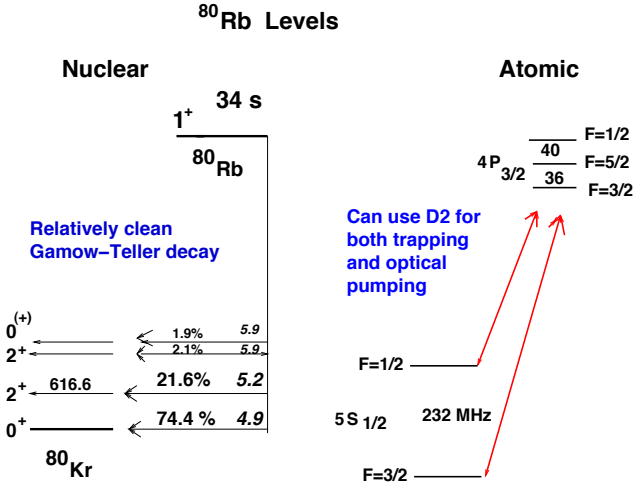

Fig. 55. ^{80}Rb nuclear and atomic level schemes.

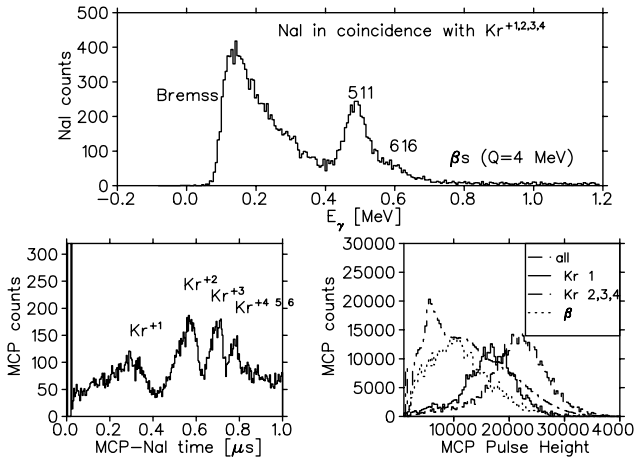

Fig. 56. NaI energy spectrum, time-of-flight spectrum from NaI-MCP coincidences, and singles pulse height spectrum in the MCP for various types of events. See text.

Also shown is a typical TOF spectrum of the recoils in coincidence with all MCP events. The various ion charge states produced in the β^+ decay are separated by the electric field. The third part of the figure shows the MCP pulse heights for the various types of events, as determined with the NaI coincidences. High pulse heights are dominated by Kr ion recoils, so a cut on pulse heights can suppress backgrounds from βs and γs.

Polarization and trap motion systematic Our analysis of ^{37}K data was made very difficult by this effect. In Expt. 715, we switched off the MOT quadrupole coils as well as the trap laser light, with 2 ms off/on duty cycle. We optically pumped during the cloud expansion to polarize the atoms. The atom cloud expands from 2 to 4 mm FWHM in this time. We can measure this in all 3 dimensions by photoionizing a small fraction of the atoms with a pulsed 355 nm laser and measuring their position and TOF information with the MCP. The analysis is complicated by the small number of trapped atoms, and a systematic error is introduced.

For Expt. 956 such a systematic error would go directly into the asymmetry and not be suppressed by the vanishing observable. So we chose to minimize it by switching the MOT off for 20 μs, which does not allow the atoms to expand. We must leave the MOT 10 G/cm quadrupole field on to do this, and optically pump in the presence of this field. We have achieved 80% polarization in ^{37}K in the past by this method, which would be adequate for the vanishing observable in Expt. 956.

We successfully measured the trap motion systematic. The trap shifted by 0.51 ± 0.02 mm between σ^+ and σ^- optical pumping light. This produces a false $\Delta A_{\rm recoil} = 0.0100 \pm 0.0004$.

The polarization achieved, however, was only 0.55 ± 0.11, as measured by asymmetries of β-MCP coincidences using the NaI and the additional CaF detectors. The earlier ^{37}K 80% polarization was achieved in the horizontal plane of the MOT quadrupole field, so displacing the atoms horizontally by unbalancing the MOT beams produces a local B field that points toward the origin. The mistake we made was to optically pump instead along the 30° axis determined by the CaF detectors. In the future we will either pump horizontally (sacrificing accuracy in the CaF detector asymmetries, which are not essential to Expt. 956) or we can optically pump with the MOT off as in Expt. 715.

Data were taken that would determine $A_{\rm recoil}$ to 0.01 statistical error. Analysis is proceeding to quantify systematic errors from the background in the MCP, as well as a subtle effect caused by saturation of the position-determining resisitive anode data.

Future In December we received EEC approval for shifts to complete data-taking for this experiment. This experiment constitutes the main component of the M.Sc. for students R. Pitcairn and D. Roberge, UBC.

Experiment 964
TACTIC – TRIUMF annular chamber for tracking and identification of charged particles
(G. Ruprecht for the TACTIC collaboration)

TACTIC is a cylindrical ionization chamber for the detection of ejectiles from nuclear reactions. It allows the three-dimensional reconstruction of particle tracks by means of a two-dimensional anode array combined with a time-of-flight measurement of the drift electrons. For more details see the TACTIC Web site: http://tactic.triumf.ca.

One key element of TACTIC is a gas electron multiplier (GEM) foil [Sauli and Sharma, Ann. Rev. Nucl. Part. Sc. **49**, 341 (1999); Sharma and Sauli, Nucl. Instrum. Methods **A350**, 470 (1994)] which acts as a preamplifier inside the chamber and therefore provides low-noise signals requiring only one further stage of amplification. In order to determine the operational parameters of this relatively new device a planar test chamber including a 5 MeV α particle source has been assembled. Different gas mixtures have been applied and the signals were measured with the results shown in Fig. 57. It was found that a 90% helium–10% CO_2 gas mixture (as required in the ^{8}Li$(\alpha,n)^{11}$B experiment, see below) is very well suited to achieve a high gain.

The test chamber has a drift volume of about $20 \times 20 \times 2\,\mathrm{cm}^3$ and an active GEM area of $8 \times 8\,\mathrm{cm}^2$, covering 16 active anode strips with 5 mm width each.

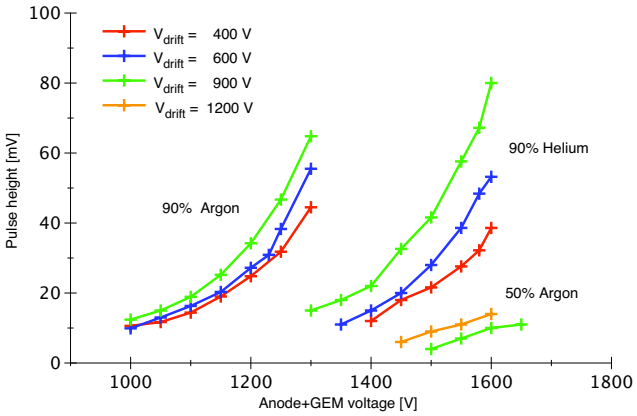

Fig. 57. Pulse heights vs. GEM+anode voltage. The GEM voltage is a factor of 3.3 smaller.

Measuring the time differences between the signals on 4 consecutive strips, we have been able to gain a projected image of the particle tracks, as can be seen in Fig. 58. The source was 5 cm before the first strip but due to a missing trigger the tracks are normalized to the first strip.

In a second phase a gas handling system has been set up. This allows a continuous regulation of the pressure down to 100 mbar while keeping the He-CO_2 mixture at a constant ratio (below 100 mbar the oxygen contamination becomes too high and quenches the signals) and the flow rate at 200 cm^3/min. This enabled the dependence of the GEM gain on the pressure and the applied GEM voltage to be determined.

The geometry for the planar as well as for the cylindrical chamber has been entered in the particle simulation program GEANT4 which allows a better separation of geometrical side effects from the actual physics. The simulated spectra are in good agreement with the test chamber measurements. Particle track simulation

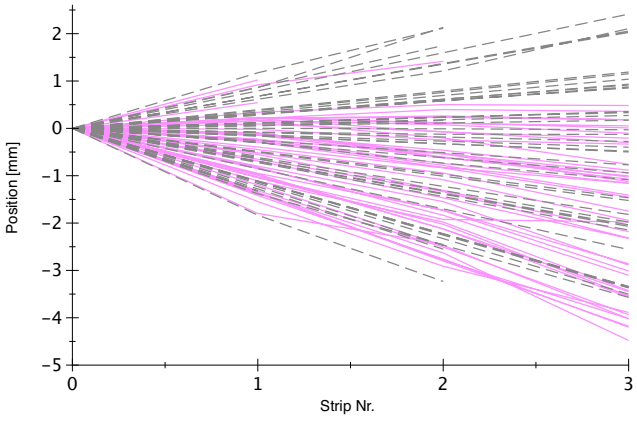

Fig. 58. Electron drift times w.r.t. the first strip, converted to distances assuming a drift velocity of 12 mm/μs. The electrons are released along the tracks of the α's. The dashed lines stem from a GEANT4 simulation, the solid, purple lines from the measurement.

for the cylindrical chamber is and will be an indispensable tool for the design of the prototype chamber. The process will involve modifying the low energy stopping algorithm of GEANT4 to give accurate ranges for heavy ions, an effort which will result in a contribution to GEANT4 development.

For a precise calculation of the electrical drift field and fringe effects of the chamber end-caps, we are using the FEMLAB code which can model the field of the chamber in 3 dimensions. A two dimensional code, GARFIELD, has been used to model the field in the target region to investigate the beam ionization problem; electrons produced in the target region can drift into the tracking region of the chamber. It was found that a cylindrical ring of guard wires at slightly higher potential than the cathode wires would eliminate the unwanted electrons.

For the data acquisition we will use a 48 channel flash-ADC VME board. The pulses will be sampled with a rate of 10–100 MHz and the required time and charge information will be extracted in real time by a user-defined algorithm in the on-board firmware. For the collection, storage, and on-line analysis of the data we will use the TRIUMF DAQ packages, MIDAS and ROME (see http://midas.triumf.ca).

TACTIC is useful in particular for experiments with gas targets and low-energy ejectiles that cannot penetrate a gas cell window, or for experiments with a high number of background particles that cannot be separated by conventional methods. The first planned experiment is the measurement of the ^{8}Li$(\alpha, n)^{11}$B reaction. Since helium can be used very well as a detector gas in combination with a GEM, no separation foil between target and detection region is necessary and the low-energy ^{11}B recoils can easily pass out of the target through the cathode wires and into the drift region to be tracked.

Other planned experiments are to measure the proton elastic scattering length on ^{7}Be which can be used to pin down the $S_{17}(0)$ value of the ^{7}Be$(p, \gamma)^{8}$B reaction, and to measure the cross section of ^{12}C+^{12}C fusion reactions which play an important role in many stellar environments.

The TACTIC collaboration: P. Amaudruz, L. Buchmann, D. Gigliotti, T. Kirchner, R. Openshaw, M. Pavan, J. Pearson, G. Ruprecht, P. Walden (TRIUMF), S. Fox, B. Fulton, A. Laird (University of York, UK).

Experiment 968
Ortho-para effect of muon catalyzed fusion in liquid deuterium
(H. Imao, N. Kawamura, K. Nagamine, KEK)

The ortho-para state of the hydrogen isotope affects resonant molecular formation in muon catalyzed fusion (μCF). Controlling the ortho-para composition is a key technique to enhancing the cycling rate of μCF. In addition, μCF experiments with ortho-para controlled deuterium provide helpful information in order to understand muonic-atomic and muonic-molecular processes. The aim of the present work is to comprehensively understand the nature of condensed-matter effects and ortho-para dependent phenomena on μCF in pure deuterium (*dd*-μCF). In *dd*-μCF, there have been some unsolved problems concerning the condensed-matter effects. An understanding of the unexpectedly high resonant molecular formation rates for solids, observed in several experiments, has not yet been achieved. Also, the ortho-para effect for solids observed by Toyoda *et al.* [Phys. Rev. Lett. **90**, 243401 (2003)] has not yet been explained by the recent theory [Adamczak and Faifman, Phys. Rev. **A64**, 052705 (2001)]. To understand these unexpected μCF phenomena in the solid phase, experiments with liquid deuterium are a key because the μCF phenomena can be observed without specific solid-state effects. We observed the dependence of *dd*-μCF phenomena on the ortho-para composition in solid, liquid and gaseous deuterium.

The main observable quantity in our experiment was a fusion neutron emitted from the $d-d$ fusion reaction, which has a monochromatic energy of 2.5 MeV. Our experiments were performed at M9B using a backward decay 52 MeV/c μ^- beam. A schematic of our experimental set-up is shown in Fig. 59. To detect 2.5 MeV fusion neutrons, four NE-213 liquid scintillators (N1–N4) were placed perpendicular to the incoming μ^- beam axis. NE-213 was chosen for its pulse shape discrimination properties. Muon-decay electrons were also detected by four pairs of plastic scintillatiors (E1–E8) placed around the target. The time spectra

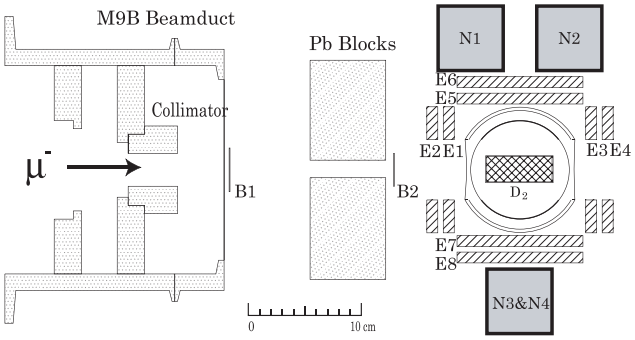

Fig. 59. Experimental set-up for solid and liquid deuterium.

of muon-decay electrons provided information about the distribution of muons stopping around the target. In addition, the number of electrons from the target was used to normalize the muon stopping number. The preparation of ortho-para controlled targets and the measurements of the ortho-para composition were essential procedures. The ortho-rich deuterium was prepared by employing a paramagnetic conversion method. In order to determine the ortho-para composition of deuterium, a rotational Raman spectroscopy method was employed for the first time in μCF. The compact Raman laser system was installed near the experimental area for *in situ* measurements. In the present study, both ortho targets and normal targets were successfully produced.

Table XI provides our results for the $dd\mu$ resonant molecular formation rate $\tilde{\lambda}_{\frac{3}{2}}$, the $d\mu$ hyperfine transition rate, $\tilde{\lambda}_{\frac{3}{2}\frac{1}{2}}$, and the non-resonant molecular formation rate, $\tilde{\lambda}_{\frac{1}{2}}$, for normal and ortho deuterium in solid and liquid phases. The decrease in the resonant molecular formation rates and in the hyperfine transition rates with ortho-rich deuterium has been observed in these phases. On the other hand, the non-resonant molecular formation rate is independent of the ortho-para state of deuterium within experimental errors. The ortho-para effect on the rates for $\tilde{\lambda}_{\frac{3}{2}}$ and $\tilde{\lambda}_{\frac{3}{2}\frac{1}{2}}$ in the solid phase is qualitatively consistent with that in Toyoda's experiment. It is worth noting that the decrease in ortho was observed even in the liquid phase, although the better resonant condition for the molecular formation process in ortho deuterium was predicted by the theory for gas. Our lower resonant molecular formation rate in liquid ortho deuterium cannot be described only by the non-thermalization effect of $d\mu$ in normal deuterium, because the experimental rates in liquid deuterium are not higher than those of the conventional theory which assumes the rapid thermalization of $d\mu$. While in the gaseous phase, the yield of the resonant fusion neutron from an ortho-rich target is significantly enhanced (Fig. 60). The ortho-para effect without condensed matter effects was observed in the gas phase. However, the neutron time spectra with gaseous ortho targets were quite strange. The unexpected bump structure was found only in neutron time spectra with gaseous ortho deuterium. The cause of this structure is not yet determined. A detailed analysis is in progress. Our experimental results will provide a breakthrough in the understanding of condensed-matter effects in dd-μCF.

Table XI. Results of the ortho-para effect on the resonant molecular formation rate, $\tilde{\lambda}_{\frac{3}{2}}$, the hyperfine transition rate, $\tilde{\lambda}_{\frac{3}{2}\frac{1}{2}}$, and the non-resonant molecular formation rate, $\tilde{\lambda}_{\frac{1}{2}}$.

T (K)	O (%)	$\tilde{\lambda}_{\frac{3}{2}}$ (μs^{-1})	$\tilde{\lambda}_{\frac{3}{2}\frac{1}{2}}$ (μs^{-1})	$\tilde{\lambda}_{\frac{1}{2}}$ (μs^{-1})
5.5	67 (2)	2.35(5)	31.6(4)	0.044(fix)
	99 (1)	1.98(5)	28.3(4)	0.043(2)
11.7	67 (2)	2.61(9)	32.0(8)	0.040(3)
	99 (1)	2.15(8)	30.1(8)	0.041(3)
18.2	67 (2)	2.46(5)	33.2(4)	0.043(2)
	99 (1)	2.11(5)	30.8(4)	0.045(2)
18.8	67 (2)	2.70(6)	32.4(4)	0.044(2)
	99 (1)	2.32(5)	30.2(4)	0.045(2)
21.2	67 (2)	2.91(8)	33.0(6)	0.048(3)
	99 (1)	2.34(7)	29.1(6)	0.046(3)
23.2	67 (2)	2.86(6)	32.6(4)	0.047(2)
	99 (1)	2.38(5)	29.8(4)	0.048(2)

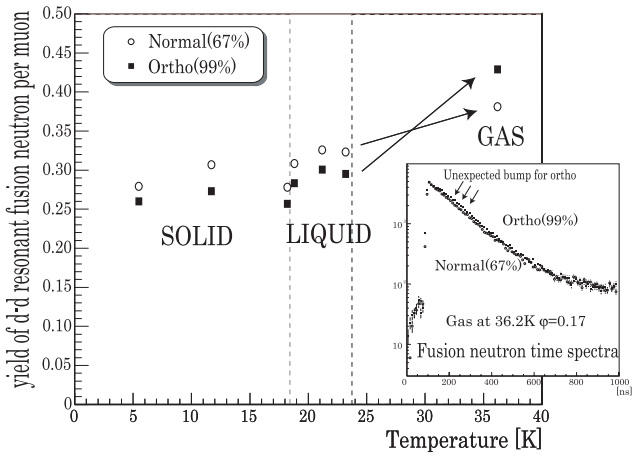

Fig. 60. The temperature dependence of the yield of fusion neutrons via resonant molecular formation.

Experiment 973
Study of coexisting collective phases far from stability: systematic decay spectroscopy of the $N = 90$ isotones
(W.D. Kulp, J.L. Wood, Georgia Tech.)

The structure of nuclei far from stability is primarily addressed using the shell model, the pairing model, and collective models. Collective models such as the model of Bohr and Mottleson [*Nuclear Structure Vol. II* (World Scientific, Singapore, 1998)], the dynamic pairing plus quadrupole model [Kumar, Nucl. Phys. **A231**, 189 (1974)], and the interacting boson model [Arima and Iachello, Phys. Rev. Lett. **35**, 1069 (1975)] have been explored extensively, but all of these models rely on parameters determined systematically from data on nuclei near stability. Further from stability, the collective structure of nuclei will be more difficult to understand as the systematic trends become less clear.

It is the goal of this experiment to map the evolution of structural trends, not only to recognize nuclear structure far from stability, but also to provide data constraining the collective models near stabil-

ity and help to discriminate between models. One of the richest regions for comparing collective models is found at $N = 90$, where the shape of the nucleus changes from nearly spherical to well deformed very abruptly as the neutron number increases from $N = 88$ to $N = 92$. In the $N = 90$ transitional region, this investigation targets the doubly-even isotones, ^{146}Ba, ^{148}Ce, ^{150}Nd, ^{152}Sm, ^{154}Gd, ^{156}Dy, ^{158}Er, and ^{160}Yb for detailed $\gamma - \gamma$, $\gamma - e^-$, and $e^- - e^-$ coincidence spectroscopy using the 8π γ-ray spectrometer and the PACES conversion-electron detector array.

A study of the β decay of ^{156}Ho to ^{156}Dy was the first stage in Expt. 973 and was the first pairing of the 8π spectrometer with the PACES array. The focus of this run was to identify excited states in ^{156}Dy populated in the decay of three isomers ^{156g}Ho ($J^\pi = 4$, $T_{\frac{1}{2}} = 56$ m), ^{156m_1}Ho ($J^\pi = 1$, $T_{\frac{1}{2}} = 9.5$ s), and ^{156m_2}Ho ($J^\pi = 9^+$, $T_{\frac{1}{2}} = 7.8$ m). Nearly 750 Gb of γ-ray and conversion-electron data were recorded in an 11 day experiment. The ^{156}Ho beam was extracted from a tantalum target and implanted onto a moving tape at the centre of the 8π spectrometer. Tape move cycles of 115 minutes, 10 minutes, and 10 seconds were used to focus on the decay of the ^{156g}Ho, ^{156m_2}Ho, and ^{156m_1}Ho isomers, respectively.

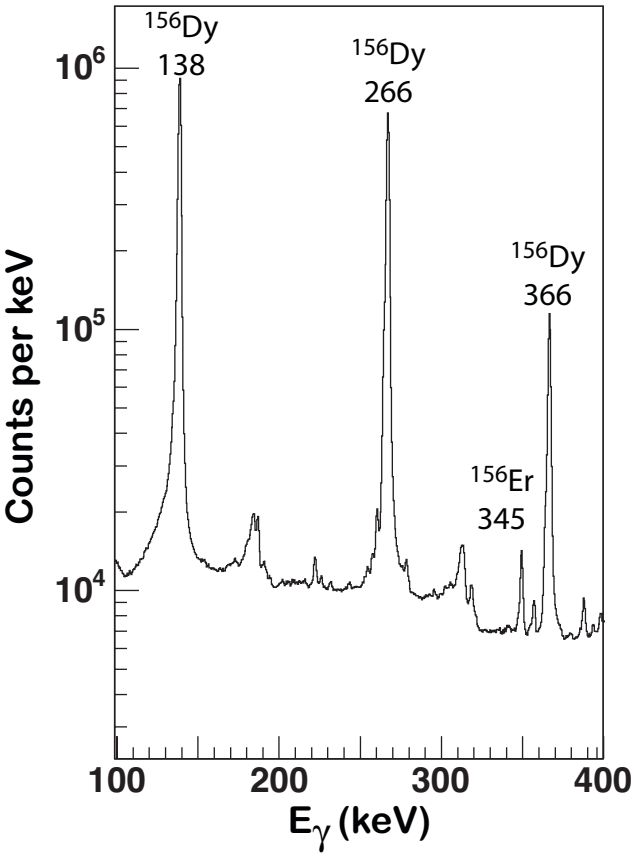

Fig. 61. γ-ray spectra from the 115 minute tape cycle reveal transitions in the ground-state band of ^{156}Dy: 138 keV ($2^+ \rightarrow 0^+$), 266 keV ($4^+ \rightarrow 2^+$), and 366 keV ($6^+ \rightarrow 4^+$) consistent with the decay of the ^{156g}Ho ($J^\pi = 4, T_{\frac{1}{2}} = 56$ m) isomer. Additional labelled transitions are associated with decays from other $A = 156$ nuclides.

Preliminary spectra reveal γ-ray and conversion-electron transitions in ^{156}Dy associated with the decays of ^{156g}Ho and ^{156m_2}Ho. Data from the 115 minute tape cycles clearly show the 138 keV ($2^+ \rightarrow 0^+$), 266 keV ($4^+ \rightarrow 2^+$), and 366 keV ($6^+ \rightarrow 4^+$) γ-ray transitions associated with the decay of ^{156g}Ho (as illustrated in Fig. 61). A spectrum from the 10 minute tape cycle (Fig. 62) shows enhanced ^{156m_2}Ho decay transitions, including the 445 keV ($8^+ \rightarrow 6^+$) γ-ray. However, other contaminating lines from other short-lived activities in the $A = 156$ chain complicate the spectrum shown in Fig. 62 and elucidation of the full decay scheme requires detailed coincidence spectroscopy.

Of particular interest in this study is the placement of weak, low-energy transitions for identification of band structures and the measurement of $E0$ transitions for interpretation of the nature of the bands. The 675 keV $E0$ transition from the first excited 0^+ to the 0^+ ground state, shown in Fig. 63, is observed in the decay of ^{156g}Ho. Thus far only an internal transition from the ^{156m_1}Ho isomer is observed with the strong decays from short-lived isobars (cf. Fig. 64), but weak decay branches may be found in further analysis with the fine tuning of timing and coincidence gates on $\gamma-\gamma$, $\gamma - e^-$, and $e^- - e^-$ coincidence events. It will be such

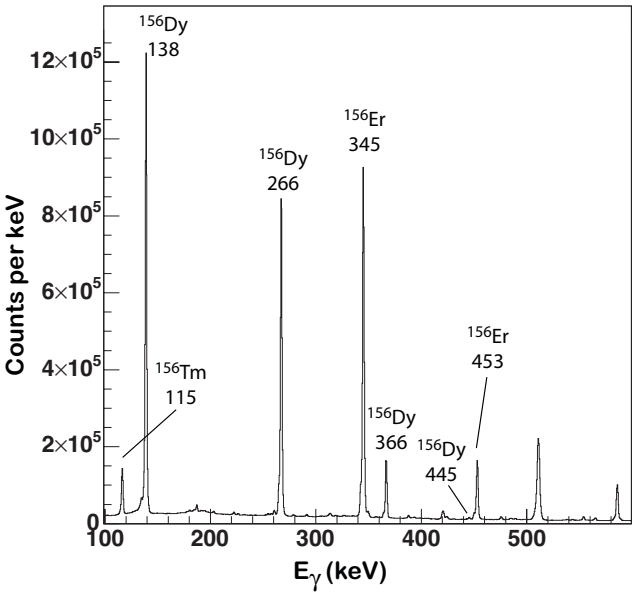

Fig. 62. The 138 keV ($2^+ \rightarrow 0^+$), 266 keV ($4^+ \rightarrow 2^+$), 366 keV ($6^+ \rightarrow 4^+$) and 445 keV ($8^+ \rightarrow 6^+$) γ-ray transitions in ^{156}Dy are highlighted using a 10 minute tape cycle, indicating the presence of the high-spin isomer ^{156m_2}Ho ($J^\pi = 9^+, T_{\frac{1}{2}} = 7.8$ m). Additional labelled transitions are associated with decays from other $A = 156$ nuclides.

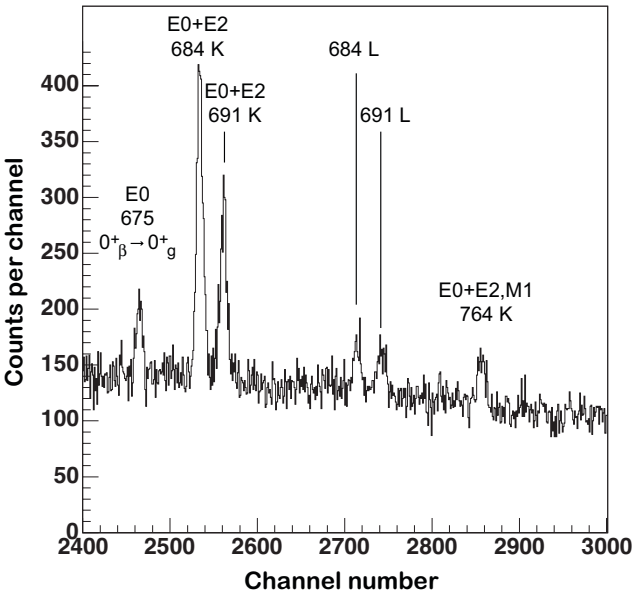

Fig. 63. The conversion electron associated with the 675 keV $E0$ transition ($0_2^+ \rightarrow 0_1^+$) observed in the decay of ^{156g}Ho to ^{156}Dy (90 minute tape cycle).

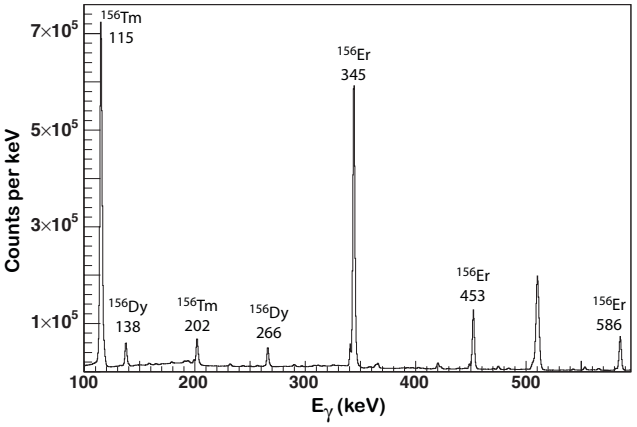

Fig. 64. While the 138 keV ($2^+ \rightarrow 0^+$) and 266 keV ($4^+ \rightarrow 2^+$) γ-ray transitions in ^{156}Dy are visible in the 10 second tape cycle, transitions associated with decays from other $A = 156$ nuclides dominate the spectrum.

detailed $\gamma-\gamma$, $\gamma-e^-$, and $e^- - e^-$ coincidence data of nuclides further from stability using the 8π spectrometer and PACES which will help discriminate between models and understand the physics of this transition region.

Experiment 973 is a collaboration of scientists from Georgia Tech., Colorado School of Mines, Lawrence Livermore National Laboratory, Louisiana State University, McMaster University, Oregon State University, Saint Mary's University, Simon Fraser University, TRIUMF, University of Guelph, University of Surrey, University of Toronto, and University of Vienna.

Experiment 984
Fast lifetime measurements with the 8π spectrometer and nuclear structure below $N = 82$
(P.E. Garrett, Guelph)

Lifetimes of nuclear levels provide crucial information on nuclear structure. Since the transition rates are determined by matrix elements of the well understood electromagnetic operator, they provide sensitive information on the charge distribution. Under the experimental program, an array of 10 BaF_2 detectors, the world's fastest scintillator, will be implemented into the 8π spectrometer to enable lifetime measurements. Experience has shown that time-delayed measurements following β decay have provided a wealth of critical level lifetimes in exotic nuclei over a wide range of nuclei in all regions of the nuclei chart. Of particular importance are studies of odd-A to locate single-particle states, and side-bands or isomeric quasi-particle states in even-even ones, that are strongly populated in beta decay but very weakly in Coulomb-excitation studies. Consequently a wide range of applications is envisaged for this timing array, with the flexibility guaranteed by a simultaneous measurement of $\beta(t) - \gamma(t) - \gamma(t)$ and $\gamma(t) - \gamma(t) - \gamma(t)$ coincidences with the Ge and BaF_2 detectors.

The array of 10 BaF_2 detectors will be mounted in available open positions on the 8π spectrometer. For standard 8π spectroscopy experiments, the time difference between the β particle detected in the plastic scintillators of SCEPTAR and the γ-ray detected in a BaF_2 detector will be used to measure lifetimes down to the sub-100 ps range. The particular decay path of the γ-ray cascade will be chosen by the high-resolution Ge detectors of the 8π. For experiments aimed at the shortest lifetimes, down to the 10 ps level, the time signal from the SCEPTAR array will be replaced with that from a single fast-plastic scintillator, mounted immediately behind the beam spot of the moving tape collector, coupled directly to a fast photomultiplier tube. These very fast lifetimes may also be measured by recording the time difference between two BaF_2 detectors, provided that the decay path can be isolated sufficiently.

As a proof of principle, a test experiment was performed in June using 4 BaF_2 detectors borrowed from the University of Surrey. A beam of ^{26}Na was delivered to the 8π spectrometer. The trigger logic was set up such that both BaF_2-SCEPTAR coincidences and BaF_2-BaF_2 coincidences could be recorded. The spectrum shows the timing of a single crystal with respect to any one of the four BaF crystals in the array. The rightmost peak in Fig. 65 is the "self timing" peak, where the same detector acts as both the start and stop for the TAC. The width of this peak indicates the

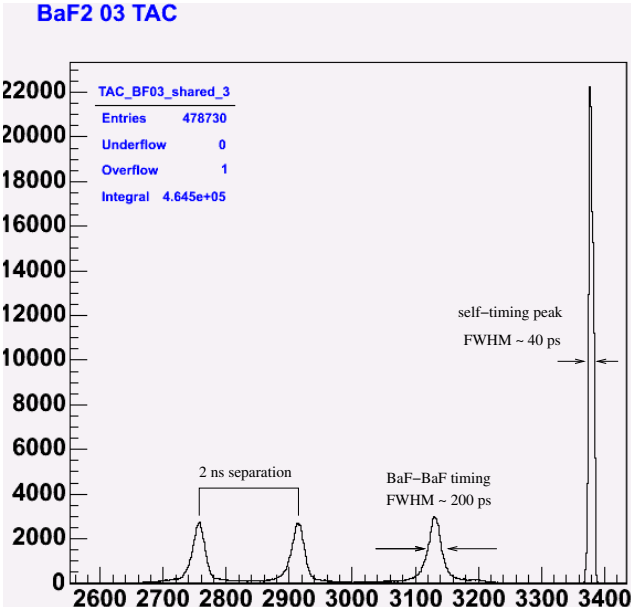

Fig. 65. Results from a test experiment using the 8π spectrometer and four borrowed BaF_2 detectors. The timing FWHM for BaF_2-BaF_2 coincidences was ≈200 ps.

amount of jitter contributed by the trigger logic for the system. The FWHM was determined to be 40 ps, which is much less than the timing resolution of the detectors themselves. The remaining peaks in this spectrum correspond to coincidences with the three other detectors, with selected delays of 3, 6 and 8 ns (respectively, left to right of the self-timing peak) for the stop pulse. The FWHM resolution for timing between separate BaF_2 crystals was ≈200 ps. Provided sufficient statistics, a precision of a few ps on the centroid position can be readily achieved.

With the addition of an array of BaF_2 detectors, the 8π spectrometer and its associated equipment will be a world-unique facility for the study of β decay in that γ-ray singles, $\gamma\gamma$ coincidences, conversion electrons, β tagging, and lifetimes can be measured simultaneously for all proposed experiments. Equipment is currently being acquired, and it is expected that the first elements of the array will be in place in the fall, 2005.

Experiment 985
Half-life and branching-ratio measurement of ^{18}Ne superallowed Fermi β decay
(M.B. Smith, TRIUMF)

Precision measurements of ft values for superallowed Fermi β decays between isobaric analogue states provide stringent tests of the electroweak standard model. Currently ft values have been measured to a precision of ±0.1% or better for nine superallowed transitions in nuclei between ^{10}C and ^{54}Co, confirming the conserved vector current (CVC) hypothesis at the level of 3×10^{-4}. These data, together with the Fermi coupling constant G_F obtained from muon-decay experiments, also provide the most accurate value for the up-down quark mixing matrix element, V_{ud}, of the Cabibbo-Kobayashi-Maskawa (CKM) matrix. Combining the V_{ud} measurement with the recommended values of V_{us} and V_{ub} from the Particle Data Group [Eidelman *et al.*, Phys. Lett. **B592**, 1 (2004)] leads to the well-known result that the sum of the squares of the three matrix elements fails to meet unity by more than two standard deviations [Hardy and Towner, Phys. Rev. Lett. (in press)]. Unitarity of the CKM matrix is a strict requirement of the standard model and the failure of this test, should the result be firmly established, would imply the need for important new physics.

A definitive conclusion on CKM unitarity can only be reached after the elimination of "trivial" explanations for the current discrepancy. For nuclear β-decay, the role of the theoretical corrections which must be applied to the experimental results has come under considerable recent scrutiny, particularly for the isospin-symmetry-breaking (Coulomb) term δ_C. The theoretical calculations can best be tested by measuring the ft values (by determining the half-lives, branching ratios and Q-values) for decays with particularly large predicted Coulomb terms or for cases where the predictions differ significantly. An example is the superallowed decay of ^{18}Ne, for which a large δ_C correction, relative to other decays with $A < 30$, has been calculated [Towner and Hardy, Phys. Rev. **C66**, 035501 (2002)]. The objective of Expt. 985 is to precisely determine the ^{18}Ne half-life and superallowed branching ratio. First beams were taken during 2004 and a precision measurement of the half-life was performed.

The technique of precisely measuring lifetimes by detecting γ-rays using the 8π spectrometer, an array of 20 Compton-suppressed HPGe detectors, is being pioneered at ISAC and has been investigated in great detail for the β decay of ^{26}Na (Expt. 909). The current measurement is the first to use this technique for a superallowed Fermi β decay. Beams of ^{18}Ne were extracted during the first development run of ISAC's electron cyclotron resonance (ECR) ion source and $\sim 4 \times 10^5$ ions/s were delivered to the 8π spectrometer for approximately 90 hours. The 30 keV beam was collected using a Mylar-backed aluminum tape, of thickness 40 μm, moving through the centre of the array. Samples were implanted for approximately four half lives and the subsequent decay was measured for ∼24 half lives before the tape was moved and the cycle repeated.

Time-stamped singles γ-ray events were recorded during the entire implantation and decay cycle for 15

runs, each run typically lasting three hours. The half-life was determined by selecting events correlated with the 1042 keV γ-ray, which follows the superallowed decay of ^{18}Ne and connects the analogue 0^+ state in ^{18}F to the 1^+ ground state. Dead-time-corrected decay curves associated with these data were fitted using a maximum-likelihood χ^2-minimization technique developed for Expt. 909 [Grinyer *et al.*, Phys. Rev. C, in press]. Experimental conditions were changed between runs in order to investigate systematic uncertainties. The 8π data acquisition system provides software-selectable pile-up and/or Compton suppression and variable (measured event by event) or fixed dead-time. These settings were varied throughout the experiment and systematic errors were also investigated by varying the shaping times of the amplifiers and thresholds of the constant-fraction discriminators. No systematic effects were found at the level of the statistical errors.

The preliminary value of the half-life of ^{18}Ne, obtained from a weighted average of the 15 runs, is 1.6676 ± 0.0016 s. This result agrees with three of the four previous half-life measurements and is five times more accurate than the currently-accepted value (1.672 ± 0.008 s) based on these determinations. After finalizing the half-life result, a publication will be submitted during 2005.

Experiment 989
Astrophysical studies using ^{26}Al ground-state and isomeric beams

(C. Ruiz, TRIUMF: for the DRAGON collaboration)

Motivation

Recent advances in space-based γ-ray astronomy have led to the mapping out of the galactic ^{26}Al distribution. The ground state of ^{26}Al is a β^+ emitter decaying to the first excited state of ^{26}Mg with a half-life of 717,000 years. This decay is then characterized by the decay of the first excited state of ^{26}Mg with a single γ-ray at 1809 keV. Because of its relatively long half-life, ^{26}Al persists in the interstellar medium long after the particular stellar cataclysm which has produced it has subsided or ended, allowing us to observe it. However, 717,000 years is a short time on the galactic star-formation timescale. The ^{26}Al distribution is then a useful indicator of the history of nucleosynthesis averaged over the last million years.

Concentrations of ^{26}Al in the galactic plane and spiral arms indicate a young, high-mass star origin of its nucleosynthesis. Candidates for this production are: core-collapse supernovae, AGB stars and classical binary-system novae. Hydrodynamic and reaction network models of supernovae and novae have produced intriguing results. The supernovae models show that 100% of the measured ^{26}Al in the galaxy can result from nucleosynthesis in the pre-collapse hydrogen-rich shell of such a star. The largest uncertainties in this model are the galactic supernova rate, the model complexity, and the nuclear reaction rates involved in the production and destruction of ^{26}Al. For novae, there is a similar uncertainty. It is still of great debate whether novae can produce a significant fraction of the galactic ^{26}Al or not. Present models say they can, however, the uncertainty in the low-temperature reaction rate of ^{26g}Al$(p,\gamma)^{27}$Si gives rise to a factor 2 uncertainty in the amount of ^{26}Al produced. The models require that this uncertainty be reduced in order to make better predictions on the nova contribution to the galactic ^{26}Al abundance that future space based γ-ray missions such as INTEGRAL will study.

At present the uncertainty in the ^{26g}Al$(p,\gamma)^{27}$Si reaction rate at nova temperatures is dominated by a single isolated resonance at $E_{cm} = 188$ keV. There has only been one direct measurement of the resonance strength of this state which has to date remained unpublished. Such a dominating resonance is required to be experimentally measured at least twice by different methods to ensure confidence in this parameter's insertion into hydrodynamic models. The previous measurement was made at Caltech in 1989 using a "traditional" (p,γ) method of impinging a low energy proton beam onto a purified radioactive ^{26}Al target and observing the γ-rays resulting from reactions using a germanium detector.

The development of intense ^{26}Al beams at TRIUMF-ISAC has provided us with the opportunity to measure the 188 keV resonance in ^{26g}Al$(p,\gamma)^{27}$Si at the DRAGON recoil separator using inverse kinematics.

Experiment

This year, DRAGON performed test studies for the ^{26}Al$(p,\gamma)^{27}$Si reaction in order to determine the feasibility of measurement of the 188 keV resonance strength. A silicon carbide target at ISAC provided an accelerated ^{26}Al beam with currents reaching a maximum of 3×10^8 particles per second, and an average of 0.7×10^8 particles per second.

The level of ^{26}Na and ^{26m}Al contaminants in the beam were monitored using a diagnostic set-up at the separator mass slits, the point where unreacted beam is deposited. Two diametrically arranged sodium iodide detectors were used to detect annihilation γ-rays from $\beta+$ decay of the 6 second lifetime decay of the ^{26}Al isomeric state, while a high purity germanium detector was used to detect the decay of the ^{26}Na via the 1809 keV γ-ray from the first excited state of ^{26}Mg. In this way, contamination levels of $0.4 \pm 0.07\%$ for ^{26}Na and $0.004 \pm 0.0007\%$ for ^{26m}Al were determined.

DRAGON's ionization chamber was used to detect particles at the end of the separator in an attempt to separate "leaky" unreacted beam particles from true recoils using $\Delta E - E$ information from the separate anode segments in the chamber. Particles were detected in coincidence with γ-ray signals from the BGO array surrounding DRAGON's windowless gas target.

Runs were taken primarily at a higher beam energy in order to see the "strong" resonance at $E_{cm} = 363$ keV. 5×10^{12} ions were received on target for this energy, and 117 ^{27}Si recoils were detected in coincidence with cascade γ-rays. The ion chamber anode information showed that at this energy, leaky beam and true recoils are just separable using the $\Delta E - E$ method (Fig. 66). ^{27}Si recoils are easily identified, however, using the time of flight round the separator between a coincident prompt γ-ray and particle detected in the ion chamber (Fig. 67). By extrapolation it was determined that recoils from the 188 keV resonance would not be separable using the $\Delta E - E$ method. A local time-of-flight system in conjunction with the separator time of flight would be necessary. Runs taken on the 188 keV resonance yielded no recoil particles because only 2×10^{13} ions were incident on target, insufficient to produce any recoils due to the low yield of 4×10^{-14} reactions per incoming ion.

The conclusions of this running period were that:

- A local time-of-flight method would be preferable in the attempt to separate recoils and leaky beam.

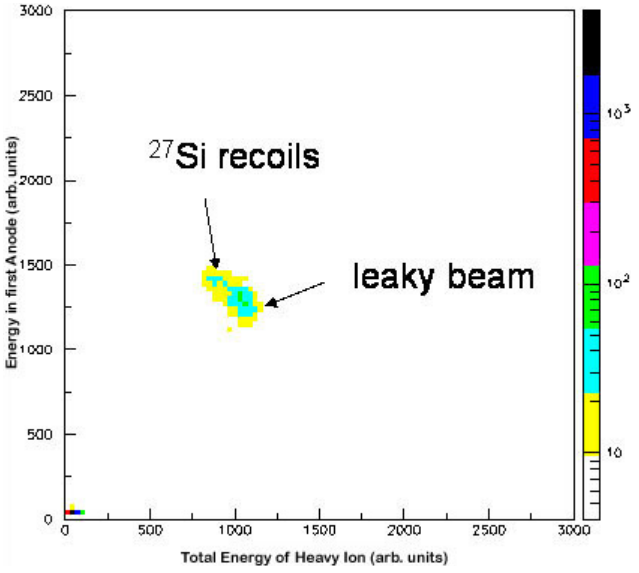

Fig. 66. Ion chamber total pulse height versus anode 1 pulse height for the ^{26g}Al$(p,\gamma)^{27}$Si reaction, showing ^{27}Si recoils and "leaky" beam.

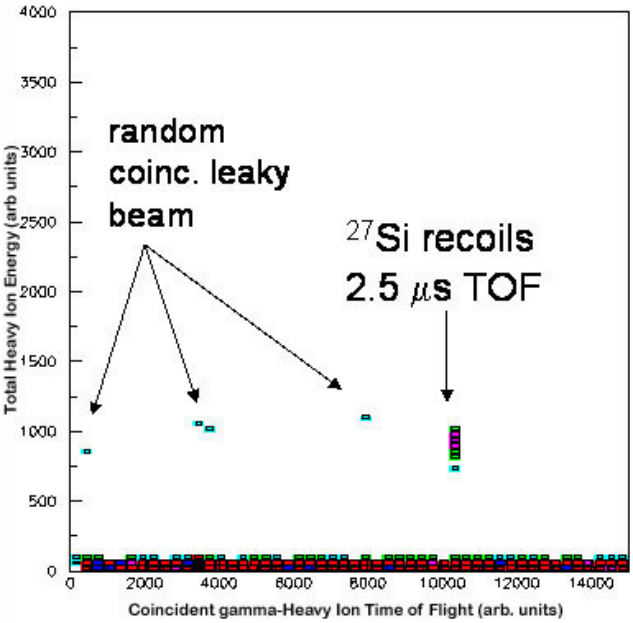

Fig. 67. Heavy ion – γ coincident separator time of flight for the ^{26g}Al$(p,\gamma)^{27}$Si reaction, showing ^{27}Si recoils and randomly coincident "leaky" beam.

- Insufficient beam intensity sustained for a reasonable duration was obtained, leading to the conclusion that a high-power silicon carbide target in combination with the TRIUMF resonant ionization laser ion source would be required to provide order of magnitude higher beam intensities.

With the improvements listed above due to be operational at ISAC over the coming year, DRAGON will attempt to make the direct measurement of the 188 keV resonance strength of the ^{26}Al$(p,\gamma)^{27}$Si in the period of running in 2005.

Experiment 992
Lifetime of the 4.033 MeV state in ^{19}Ne
(G.C. Ball, B. Davids, TRIUMF)

Novae are thermonuclear runaways resulting from the accretion of hydrogen- and helium-rich material onto the surfaces of white dwarfs in binary systems. X-ray bursts result from a similar accretion process on neutron stars, during which the temperature and density are sufficiently high to initiate breakout from the hot CNO cycles into the *rp* process, dramatically increasing the luminosity of outbursts and synthesizing nuclei up to masses of 100 u. Several reactions have been suggested as pathways for this breakout, but only two are currently thought to be possibilities: ^{15}O$(\alpha,\gamma)^{19}$Ne and ^{18}Ne$(\alpha,p)^{21}$Na. In astrophysical environments the ^{15}O$(\alpha,\gamma)^{19}$Ne reaction proceeds predominantly through resonances lying just above the ^{15}O + α threshold at 3.529 MeV in ^{19}Ne. The reaction

rate in novae is determined by the resonance strength of the 4.033 MeV $3/2^+$ state. This state may also make the largest contribution to the reaction rate at the higher peak temperatures reached in X-ray bursts.

Direct measurements of the low energy cross section, which require high-intensity radioactive ^{15}O beams, are planned at TRIUMF. Until such beams are available, the best information on the reaction rate will come from indirect measurements of the decay properties of the relevant resonances. These states lie beneath the proton and neutron separation energies, and can therefore decay only by α and γ emission. By populating these states and observing the subsequent α- and γ-decays, one can deduce the branching ratio $B_\alpha \equiv \Gamma_\alpha/(\Gamma_\alpha + \Gamma_\gamma)$. If Γ_γ is also known, one can then calculate the resonance strength and thereby the contribution of each state to the astrophysical rate of the ^{15}O(α,γ)^{19}Ne reaction. In a recent experiment at the KVI, the α branching ratios have been measured. However, experimental data on the radiative widths of these states are sparse. An effort to measure the lifetime of the 4.033 MeV state by the Doppler shift attenuation method (DSAM) resulted in an upper limit. A complementary measurement of the Coulomb excitation to this state at intermediate beam energies resulted in an upper limit on the radiative width, corresponding to a lower limit on the lifetime. The 95% confidence level allowed region for the lifetime, and therefore the reaction rate, spans two orders of magnitude. TRIUMF Expt. 992 aims to measure the lifetime of this state using the DSAM, populating it via the ^{3}He(^{20}Ne,α)^{19}Ne reaction at a ^{20}Ne beam energy of 34 MeV. A measurement of this lifetime will definitively settle the question of whether this reaction plays any role in novae, and substantially reduce the uncertainty on the reaction rate in X-ray bursts.

Preparations for the lifetime measurement are proceeding along several lines simultaneously. Implantation of Al, Zr, and Au foils with ^{3}He is being carried out at the Université de Montréal. Si surface barrier detectors have been ordered and will soon arrive. A schematic design for the cold trap and vacuum chamber assembly has been completed, and detailed designs will be completed shortly. Fabrication of the chamber can proceed promptly upon completion of these drawings. Ion optical calculations for the transport of the beam to the experiment at the end of the medium energy beam transport line have been completed and indicate a good beam spot can be achieved without any additional focusing elements. This experiment will be the subject of the master's thesis of a new UBC student, Mythili Subramanian.

EMMA

Ion optical design work has been completed for EMMA, an electromagnetic mass analyzer for ISAC-II at TRIUMF. EMMA is a recoil mass spectrometer that will be used to separate the recoils of nuclear reactions from the beam, and to disperse them according to mass/charge. ISAC-II will provide intense, low-emittance beams of unstable nuclei with masses up to 150 u and maximum energies of at least 6.5 MeV/nucleon. EMMA will be used in many different types of experiments with radioactive beams, especially those involving fusion-evaporation and transfer reactions. As such, it must be both efficient and selective, possessing large acceptances in angle, mass, and energy without sacrificing the necessary beam suppression and mass resolution.

EMMA is based on a symmetric configuration of electric and magnetic dipoles, a proven design that allows for energy dispersion cancellation. (Figure 68 schematically depicts the layout of electromagnetic components.) However, the design represents a significant improvement over existing instruments of this type. In particular, EMMA has the largest energy and angular acceptances of any recoil mass spectrometer, while simultaneously providing high mass resolving power due to the design of its quadrupole lenses and the curvature of its magnetic dipole field boundaries. This combination of large acceptance and high resolution will make EMMA the most advanced instrument of its kind. It will be an

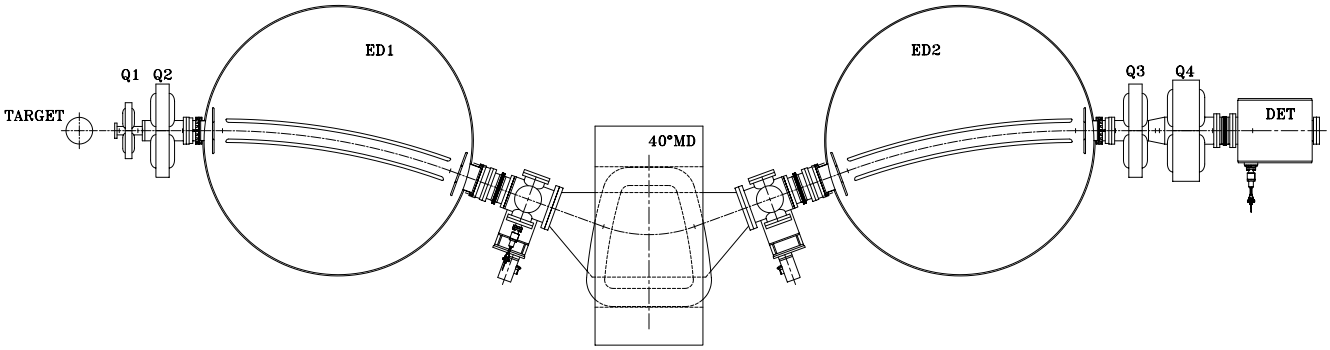

Fig. 68. Schematic view of EMMA, showing the target, quadrupole and dipole magnets, and electric dipoles. The detector box is also indicated.

indispensable part of the ISAC-II experimental facility, and will be used extensively in conjunction with the TIGRESS γ-ray detector array as well as the TUDA charged particle detectors.

The design of EMMA underwent both internal (TRIUMF) and external (NSERC) technical reviews in 2004 in order to ascertain the soundness of its ion optics as well as its suitability for the anticipated users. A paper describing the design has been accepted for publication by Nuclear Instruments and Methods in Physics Research A.

Experiment 995
An alternate approach to radioactive beam production for volatile elements
(J. D'Auria, S. Lapi, SFU)

Overview

The goal of this experiment is to demonstrate that certain radioactive beams of volatile elements, which have proven to be difficult to produce using the standard ISOL approach at the ISAC facility, can be produced using low energy protons. If successful, the produced species could be transferred in the gas phase to ISAC (either to OLIS or the on-line system), ionized using an appropriate ion source (ECR or FEBIAD) and the ionized beam accelerated to required energies using the ISAC accelerator. This approach has been successfully demonstrated at the BEAR facility at LBL [Powell *et al.*, Nucl. Instrum. Methods **B204**, 440 (2003)] and could allow ISAC to have two methods of producing beams, perhaps simultaneously (if OLIS is used). The experiment received approval at low priority in 2003 and initial studies have been performed in 2004.

Background

The proposed method of production is the irradiation of gaseous targets with 13 MeV protons using the TR13 facility. This facility (H^- cyclotron) is located in the TRIUMF accelerator building and is primarily used to produce radioisotopes for medical purposes. Possible beams available with this approach are given in Table XII along with information on target material, reaction and rate of production.

This method of production and transfer was tested in the M.Sc. study of S. Lapi who measured the production and transfer efficiency for ^{14}O [Lapi, *Development of an intense ^{15}O radioactive beam using low energy protons*, M.Sc. thesis, Simon Fraser University (2003)] using the TR13 facility.

Table XIII presents some of the beam requirements of approved ISAC experiments.

Studies in 2004

Approximately 1 Ci of ^{11}C as CH_4(g) was produced in a (p,α) reaction using the TR13. Following chemical manipulations, the active methane was hand delivered to the injection port of the on-line ECR ion source at ISAC, on two occasions. Stable methane had been injected previously into the ECR to study the operation

Table XII. Calculated production rates in a target using 50 μA of 13 MeV protons (TR13).

Isotope	Half-life	Target material	Production reaction	Saturation rate of production
^{11}C	20.3 m	$^{14}N_2$ (g)	$^{14}N(p,\alpha)^{11}C$	2.4×10^{11}/s
^{14}O	70.6 s	$^{14}N_2$ (g)	$^{14}N(p,n)^{14}O$	2×10^{10}/s
^{15}O	122.2 s	$^{15}N_2$ (g)	$^{15}N(p,n)^{15}O$	2.1×10^{11}/s
^{13}N	9.97 m	O_2 (g)	$^{16}O(p,\alpha)^{13}N$	4.8×10^{10}/s
^{18}F	1.83 h	Enriched ^{18}O (g)	$^{18}O(p,n)^{18}F$	5.2×10^{11}/s
^{17}F	64.5 s	Neon gas	$^{20}Ne(p,\alpha)^{17}F$	1.5×10^{11}/s

Table XIII. Beam requirements for ISAC experiments approved or to be presented.

Beam	Experiment #	Optimal intensity	Minimum intensity
^{11}C	new	$10^{8,9}$	
^{14}O	924	10^6	5×10^5
^{15}O	813	10^{11}	10^{10}
^{15}O	900	10^9	10^8
^{13}N	805	10^9	10^8
^{17}F	946	10^9	10^8
^{19}Ne	811	10^8	10^7

of the source for ionizing methane, e.g. the optimal ion was CH_3^+. A NaI(Tl) gamma detection system was set up at the ISAC collection station (on the mass separator floor), and a stable beam was optimized onto the FC positioned just before this station. The result of these two studies was not completely successful. While there was an indication of ^{11}C possible activity at the collection station (10^4 cps), this represented an overall efficiency of ∼0.01%. This includes but is not limited to decay losses prior to the observation, losses due to the transfer through a mass transfer value prior to the ECR, the ECR efficiency, beam tuning transmission losses and perhaps others. Apparently most of the activity did not make it into the ion source efficiently but seemed to remain in the gas inlet system prior to the source. While the exact cause of this is not clear, nevertheless, the manipulations with the ECR were useful and may have played a role in the ultimate successful operation of this new system. It should be noted that the tests for Expt. 995 were limited to a narrow one week window during which the ECR was available for such types of tests, in order not to interfere with its use for RB production for experiments.

A series of tests are planned for 2005 at the off-line ECR test system (essentially the same ECR source). Initial studies will use a $^{13}CO_2$ gaseous source to understand the ionization efficiency of the ECR for CO_2. In addition a series of gaseous dilutions will be studied which will attempt to mimic the concentrations of ^{11}C in an actual production cell. Following these tests, approval will be sought to perform some low activity tests with an actual ^{11}C production cell in order to fully understand this system prior to seeking time with the on-line system.

Experiment 1008
A new look at the β-decay of ^{11}Li
(F. Sarazin, Colorado School of Mines)

Last year, a measurement of the ^{11}Li yield out of a tantalum target reached a record breaking 44000 ^{11}Li per second, making TRIUMF/ISAC the facility delivering the most intense ^{11}Li beam in the world. Following an already successful measurement of the β-decay of ^{11}Li in August, 2002 [Sarazin *et al.*, Phys. Rev. **C70**, 031302(R) (2004)], the time was right to investigate again the complex decay of ^{11}Li, using the enhanced ^{11}Li yield available and also utilizing the new addition to the 8π: SCEPTAR, an array of 20 plastic scintillators allowing the detection of β-γ coincidences. The experiment took place in October. A beam of about 15000 pps was delivered to the 8π and implanted on an aluminum foil at the centre of the 8π/SCEPTAR arrays. Most of the ^{11}Li β-decay strength is observed to proceed through unbound states in ^{11}Be, which subsequently decay by one-neutron emission to ^{10}Be. This results in the observation of a γ-spectrum dominated by the decay of the excited states in ^{10}Be. These transitions exhibit characteristic Doppler-broadened lineshapes, due to the recoiling effect induced by the neutron emission. The main objective of this measurement was, by means of lineshape analysis, to look for weak branches in the β-delayed one-neutron emission to excited states in ^{10}Be. In particular, good statistics are required to determine the precise lineshape of the 5.96 MeV peak, which is crucial to resolve unanswered questions left from the first experiment. Moreover, some results of the first analysis are in disagreement with results reported recently by Hirayama *et al.* [Phys. Lett. **B611**, in press] on another experiment performed at TRIUMF/ISAC, using a polarized ^{11}Li beam and neutron detectors. About 15 times more data were obtained with an improved signal to background ratio due to the measurement in β-γ coincidences. This ratio was further improved by the rejection of bremsstrahlung events, e.g. high-energy electrons slowing down in the plastic scintillators and emitting one or more γ-rays in the forward direction, firing the nearby germanium detector (see Experimental Facilities: 8π Spectrometer, this Annual Report). The improvement in the lineshape quality is particularly impressive for the 5.96 MeV peak, as can be seen in Fig. 69.

The improved statistics obtained in this experiment also allowed us to look at γ-γ coincidences. The lineshape of the 2.59 MeV and 5.96 MeV peaks results from the decay of a doublet of states (1^-, 2_2^+) in ^{10}Be only 1.7 keV apart. The sharp contribution originates from the decay of the relatively long-lived second 0_2^+ state to the 1^- state in ^{10}Be located at 6.180 MeV. By

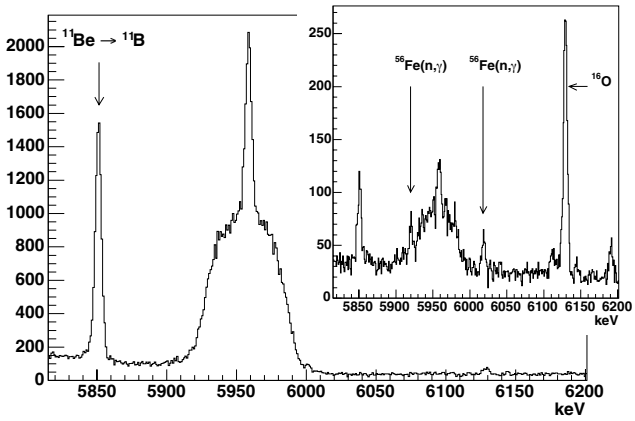

Fig. 69. Compton suppressed γ-spectrum following the β-decay of ^{11}Li. The lineshape of the 5.96 MeV peak obtained in β-γ coincidence with bremsstrahlung correction is shown. The lineshape obtained in the first experiment is shown in the inset. One can see that background γ-ray lines, unrelated to the β-decay of ^{11}Li, have disappeared in the new spectrum.

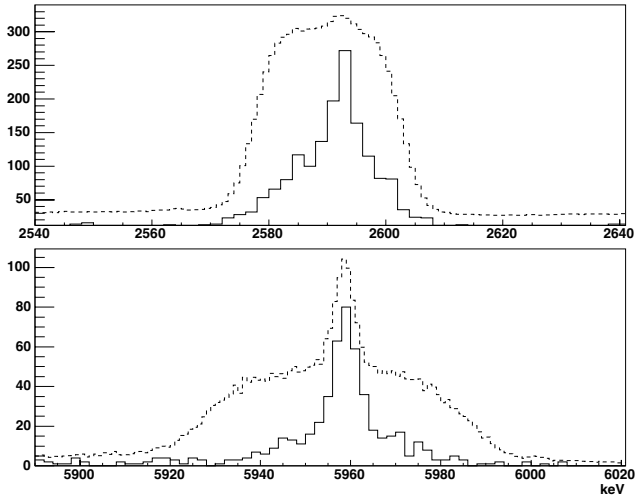

Fig. 70. γ-γ coincidences gated with the 219 keV $0_2^+ \rightarrow 1^-$ transition. The sharp component is singled out by the coincidence (continuous line) and is shown together with the scaled-down original lineshape at 2.59 MeV (top) and 5.96 MeV (bottom).

gating on the 219 keV transition linking both states, it is possible to isolate this sharp contribution, as seen in Fig. 70.

More analysis is in progress to actually fit the various lineshapes with a Monte Carlo simulation developed during the analysis of the first measurement. This will be the main body of the Ph.D. thesis of Caleb Mattoon at the Colorado School of Mines.

LANSCE Experiment NPDGamma
Measurement of the parity-violating gamma asymmetry A_γ in the capture of polarized cold neutrons by para-hydrogen, $\vec{n} + p \rightarrow d + \gamma$

(S.A. Page, W.D. Ramsay, Manitoba)

Introduction

The $\vec{n} + p \rightarrow d + \gamma$ experiment had a very successful commissioning run from February to April. All the equipment except the liquid hydrogen target was successfully commissioned during the run. It was intended to install the liquid hydrogen target during the summer of 2004, with another data-taking starting again in the fall, but a site-wide "stop work order" at Los Alamos National Laboratory put all work not related to security or safety on hold and normal activities were very slow to resume. We now expect the liquid hydrogen target to be commissioned in late 2005. A Manitoba M.Sc. student is now completing his thesis on work performed for the 2004 commissioning run.

The $\vec{n}p \rightarrow d\gamma$ collaboration involves 13 institutions, with Canadian collaborators from the University of Manitoba, and infrastructure support from TRIUMF. The authors of this report, S.A. Page and W.D. Ramsay, took responsibility for precision monitoring of the neutron beam flux, and designed a new current mode beam monitor that was first tested in the fall of 2001 at LANSCE. Three additional beam monitors based on this new design were subsequently constructed and used with great success in the 2004 commissioning run. Canadian participation in $\vec{n} + p \rightarrow d + \gamma$ includes vital infrastructure support from TRIUMF on the design and construction of a computer controlled motion system for the gamma detector array and liquid hydrogen target to be used for calibration of the effective detector alignment *in situ*. This procedure requires that the entire one-tonne detector array be moved accurately in the vertical and horizontal directions by up to ± 5 mm. TRIUMF also designed and built custom VME modules that permit the gain of each of 48 detector channels to be adjusted under computer control. A prototype was tested at Los Alamos in 2003 and 6 more were built at TRIUMF in 2004 and delivered to Los Alamos.

The experiment is designed to measure the very slight up-down asymmetry, A_γ, in the capture of vertically polarized cold neutrons on liquid parahydrogen. If parity is conserved in the reaction, A_γ will be zero. The reason for doing this is that it provides a very clean measure of the weak pion nucleon coupling, f_π^1. In fact, to a very good approximation, $A_\gamma = -0.11 f_\pi^1$. The value of f_π^1 is somewhat controversial [Wilburn and Bowman, Phys. Rev. **C57**, 3425 (1998)]. The experimental and theoretical situation is summarized in Fig. 71. ^{18}F gamma circular polarization experiments give zero. Haxton interprets the results to indicate $f_\pi^1 = 0 \pm 1.0 \times 10^{-7}$ [Ann. Rev. Nucl. Part. Sci. **35**, 501 (1985)]. The ^{133}Cs anapole moment, on the other hand, gives a non-zero value. Flambaum interprets the result

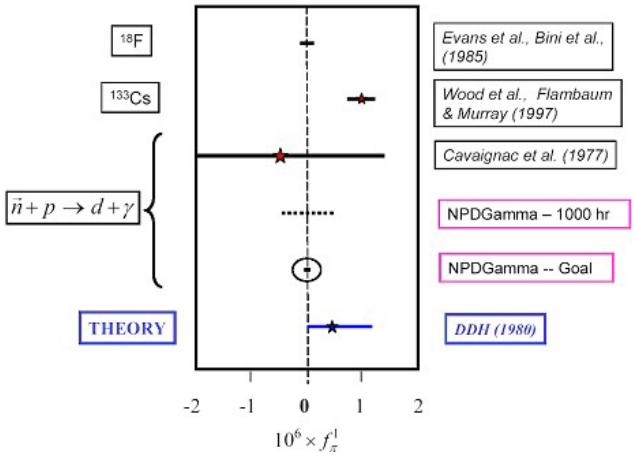

Fig. 71. Experimental and theoretical limits on the weak pion-nucleon coupling f_π^1. The expected precision of an initial run of the NPDGamma experiment at LANSCE, assuming 1000 hours of data, is shown, as is the statistics-limited final result planned for the experiment.

to give $f_\pi^1 = 7 \pm 3 \times 10^{-7}$ [Phys. Rev. **C56**, 1641 (1997)]. Because NPDGamma is based on a simple two-nucleon system without the complex many-body dynamics of the ^{18}F and ^{133}Cs experiments, the LANSCE experiment has a good chance of laying this controversy to rest. The goal of the experiment, as indicated in Fig. 71, is to measure f_π^1 to $\pm 0.5 \times 10^{-7}$, which is approximately 1/10 of the mid-range theoretical estimates. The "1000 hour" point in Fig. 71 is based on test run results [Mitchell *et al.*, Nucl. Instrum. Methods **A521**, 468 (2004)] and shows the uncertainty we might reasonably expect to achieve in the first data run with hydrogen at LANSCE, which is expected in 2006.

The NPDGamma experiment

The experiment set-up at LANSCE is shown schematically in Fig. 72. An 800 MeV proton beam pulsed at 20 Hz impinges on a tungsten spallation target; MeV neutrons emerging from the target are cooled in a liquid hydrogen moderator and transported via a supermirror guide to the experimental apparatus, where they emerge from the (9.5×9.5) cm^2 guide at 21 m from the source. The m = 3 supermirror guide enhances the total neutron flux in the desired energy range 0–15 meV with respect to the Maxwellian distribution of neutrons emerging from the moderator. The pulsed nature of the beam enables the energies of the neutrons to be determined from their times of flight, which is an important advantage for diagnosing and reducing many types of systematic error. Neutrons are polarized in the vertical direction by selective transmission through a polarized ^{3}He gas cell which acts as a spin filter, producing an energy dependent polarization spectrum.

The three beam monitors (marked "Monitor" in Fig. 72) are ^{3}He ionization chambers provided by the University of Manitoba collaborators, supported by NSERC. In Fig. 73, two of these monitors are shown mounted for testing at the start of the 2004 commissioning period at Los Alamos. The three monitors measure the neutron beam intensity upstream and downstream of the polarizer cell, and at the end of the beam line. The transmission of the ^{3}He cell serves as an on-line measurement of its polarization and hence that of the neutron beam, and the transmission through the liquid hydrogen target is an on-line monitor of the orthohydrogen/parahydrogen ratio in the target.

A uniform vertical guide field, $B_o = 1$ mT, preserves the neutron beam polarization as it is transported to the liquid hydrogen target, where the incident neutrons are captured to produce the 2.2 MeV γ-rays of interest. Low energy neutrons depolarize rapidly in orthohydrogen, while those below 15 meV retain their polarization in a parahydrogen target; hence, it is important to ensure that the liquid hydrogen target is prepared and maintained with the very low equilibrium orthohydrogen concentration of 0.1%. By placing monitors before and after the target, the ortho-hydrogen concentration can be monitored on-line, since the scattering cross sections for ortho- and para-hydrogen differ by about a factor of 20 in the energy range of interest. Approximately 60% of the beam neutrons will be captured in the target.

The 2.2 MeV γ-rays from neutron capture in the target are detected with an array of 48 $(15 \times 15 \times 15)$ cm^3 CsI(Tl) crystals surrounding the target. The detectors are read out in current mode by vacuum photodiodes coupled via low noise current-to-voltage preamplifiers to transient digitizers sampling the diode signals every 10 μs. A resonant radio frequency (rf)

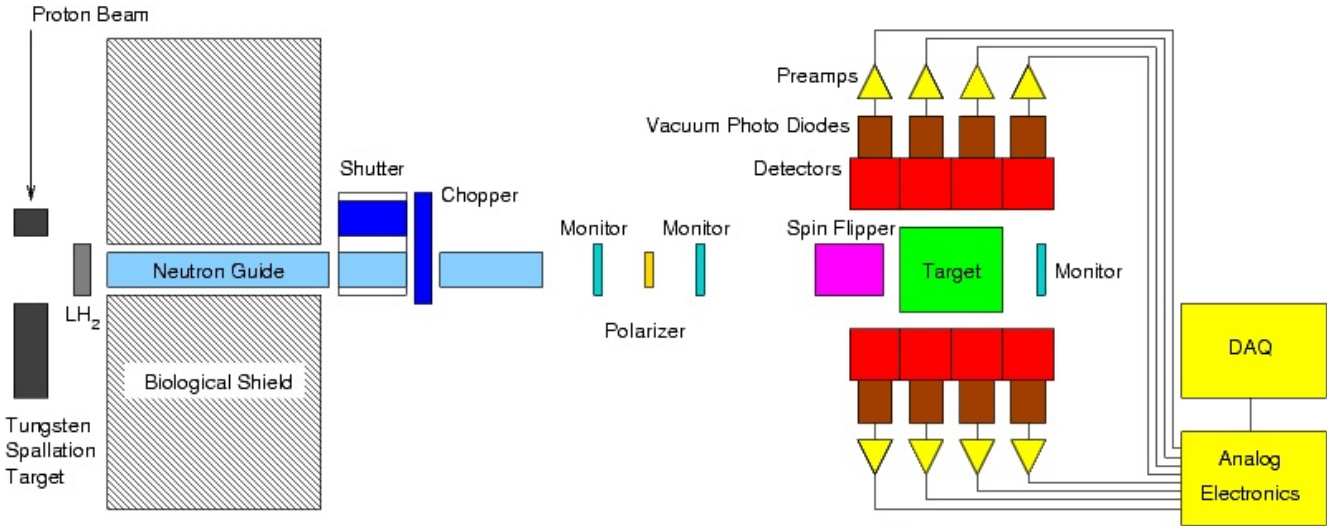

Fig. 72. Schematic of the NPDGamma apparatus on flight path 12 at LANSCE.

Fig. 73. Manitoba ^{3}He neutron monitors installed on FP12 near the start of the 2004 commissioning run. Later in the run, the monitors were used to measure neutron flux, neutron polarization, and spin flip efficiency.

spin flipper, consisting of a 30 cm diameter by 30 cm long solenoid whose magnetic field amplitude is tailored as a function of time of flight to flip neutron spins of all energies, is located upstream of the target. The spin flipper reverses the direction of the neutron spin on successive beam pulses according to an 8-step $[+--+-++-]$ reversal pattern, which cancels systematic drifts of detector efficiencies and electronic gains to second order. The spin flipper efficiency has been measured in tests runs to be in excess of 98% across a large area as appropriate to the beam size in our experiment.

The statistical uncertainty in the measurement of A_γ is ultimately determined by counting statistics, set by the beam intensity, the detector solid angle, and the counting time. Care has been taken to identify all possible sources of error, to minimize the sensitivity of the apparatus, and to work out a program of ancillary measurements to quantify individual error sources. The overall conclusion of these studies is that it should be possible to measure A_γ to $\pm 0.5 \times 10^{-8}$ with systematic errors no larger than 10% of the statistical error quoted above. Several key features of the experimental design should be noted here, namely:

1. three independent magnetic field reversals can be employed to manipulate the neutron spin and should give identical results for A_γ (^{3}He cell, rf spin flip, holding field in the experimental area);

2. the pulsed beam allows systematic effects to be isolated by their different time-of-flight dependences;

3. the use of vacuum photodiodes for detector readout reduces the gain sensitivity to magnetic fields as compared to conventional photomultiplier tubes by 4 orders of magnitude, and the detector gains are essentially independent of bias voltage;

4. the depolarization of the beam above 15 meV allows a number of systematics associated with interaction of polarized neutrons in the target to be isolated;

5. the very small value of the electronic noise compared to counting statistics (1/100) makes it possible to test for instrumental effects with a standard uncertainty of 10^{-9} on a timescale of one day.

Systematic errors arising from interactions of the neutron spin are potentially the most serious for the experiment. Spin dependent effects can lead to either up-down or left-right asymmetries which could leak into the up-down signal from which A_γ is deduced. To limit contributions from left-right asymmetries at or below 5×10^{-10}, we require a means of determining the detector alignment with respect to the neutron spin direction to 20 mrad or better. To accomplish this, TRIUMF, in collaboration with the University of Manitoba, has designed and built a computer controlled detector stand capable of moving the entire 1000 kg CsI array by a few millimetres horizontally and vertically with the target in place. The effective position of each detector can be determined by the γ yield in that detector as a function of the array position. Figure 74 shows the array in place on the TRIUMF/Manitoba motion controller.

Fig. 74. CsI array mounted on the Manitoba/TRIUMF detector motion stand in the NPDGamma cave. The 1000 kg detector can be moved ± 10 mm in x and y under computer control.

Progress toward data-taking

The new FP12 beam line for NPDGamma was completed late in 2003, and the experimental apparatus, exclusive of the liquid hydrogen target, was installed in the new FP12 cave early in 2004 (Fig. 74). We have just completed a very successful first commissioning run, during which the beam line, chopper, beam monitors, magnetic guide field, ^{3}He polarizer and analyzer cells, rf spin flipper, full CsI detector array and data acquisition systems were exercised. Following a tune up and commissioning of each element of the apparatus, time was devoted to measurements of parity violating asymmetries from solid targets that will contribute to backgrounds in the NPDGamma measurements, e.g. from the aluminum target vessel, and measurements with a boron target were used to confirm that the full array operates at the counting statistics limit. Highlights of the commissioning run are discussed briefly below.

A very important demonstration was that the electronic noise was insignificant compared to counting statistics. Figure 75 compares the electronic noise to the counting statistics. One sees that the detector electronics performed well and that the electronic noise is indeed small.

The neutron guide and frame overlap chopper were also commissioned. Figure 76 shows the measured neutron time-of-flight distribution using the ^{3}He ionization chamber mounted at the end of the flight path 12 neutron guide. Agreement with the Monte Carlo calculation as normalized to the measured moderator brightness is excellent. Ultimately, the FP12 neutron flux will limit the precision in A_γ that we can obtain in a reasonable amount of running time at LANSCE.

The experimental counting rate asymmetry is given by $\epsilon = P_n A_y$ where P_n is the beam polarization; the performance of the ^{3}He spin filter cell therefore has a crucial influence on the statistical precision of the A_γ result. With precision beam monitors located upstream and downstream of the ^{3}He polarizer cell, the neutron beam polarization can be inferred directly from a comparison of the polarized and unpolarized cell transmissions – this allows for a continuous on-line measurement of the neutron beam polarization during NPDGamma data-taking. An example under commissioning run conditions (the ^{3}He polarization was not yet fully optimized) is shown in Fig. 77. It is worth noting that, with the spin filter technique, the neutron polarization can be considerably more than the ^{3}He polarization.

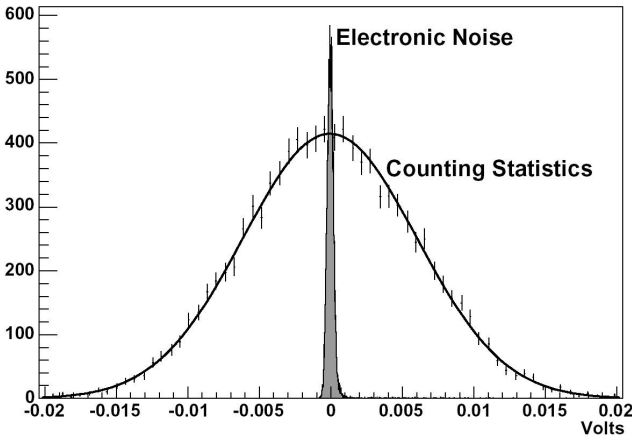

Fig. 75. Performance of the detector electronics during the commissioning run. Electronic noise alone is insignificant compared to counting statistics.

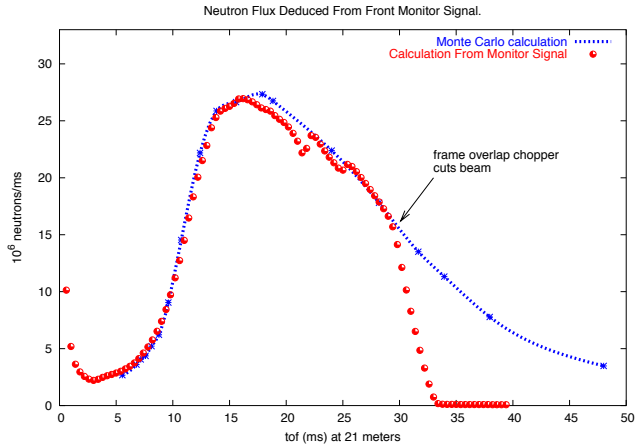

Fig. 76. Neutron time-of-flight distribution at the exit of the neutron guide compared to a Monte Carlo calculation. The large red dots are measured by the first Manitoba monitor and the small blue dots are a Monte Carlo calculation. The measured time-of-flight distribution falls off sharply around 30 ms when the frame overlap chopper enters the beam. The two sharp dips near the peak of the curve are Bragg edges from aluminum in the beam.

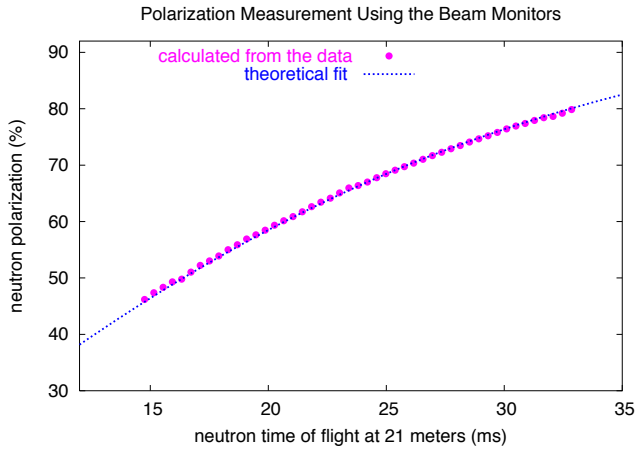

Fig. 77. Polarization measured with the Manitoba beam monitors during the 2004 commissioning run. By measuring the transmission through the ^{3}He cell with the cell polarized and unpolarized, the absolute neutron polarization can be determined without knowing the ^{3}He polarization.

During the commissioning run, we repeated our earlier measurements of the parity violating up-down γ asymmetry following neutron capture on ^{35}Cl and confirmed the earlier results to much higher precision in a few hours of integration time. The NPDGamma detector array is such a precise instrument that we were able to use this small parity-violating asymmetry to tune the rf spin flipper, although use of a polarized ^{3}He analyzer cell and a third beam monitor downstream of the cell is the preferred method. During NPDGamma data-taking, we plan to periodically measure this asymmetry with a Cl target to monitor the consistency of the detector performance.

To study a possible background, we also measured the asymmetry using a solid aluminum target. The CsI detector array performed superbly. The γ-ray asymmetry histogram was Gaussian over at least 4 orders of magnitude, with only very loose cuts on the incident neutron beam intensity. The conclusion from this preliminary analysis is that the parity violating asymmetry following neutron capture on aluminum is small enough that it will result in a negligible background correction with the liquid hydrogen target running.

Summary and future outlook

The NPDGamma experiment has just completed a very successful first commissioning run on flight path 12 at LANSCE. We have demonstrated that the full CsI detector array, instrumented for current mode readout, achieves a statistical error consistent with counting statistics. In late 2005, the liquid hydrogen target will be installed, followed by first data-taking as soon as possible, probably during the 2006 run cycle. We have determined that the physics asymmetry A_γ can be measured at LANSCE with the full NPDGamma apparatus with a statistical error of $\pm 4 \times 10^{-4}$ per beam pulse with 120 μA proton beam on the spallation target – unfortunately this falls short of our original $\pm 1 \times 10^{-4}$ per beam pulse goal that would enable us to measure A_γ to 10% of its predicted value in one calendar year of running time. Our test measurements have shown that expectations of the available neutron flux from the upgraded LANSCE facility were too optimistic by almost a factor of 4, with roughly equal contributions from reduced moderator brightness and reduced production beam current.

In view of the ultimate limit on the statistical accuracy that we can hope to achieve at LANSCE, the NPDGamma collaboration plans to complete commissioning of the apparatus and carry out a first measurement in 2006, which would provide a statistics-limited result for A_γ accurate to a standard uncertainty of 5×10^{-8} or better, improving on existing measurements in the neutron-proton system by a factor of 4, as shown in Fig. 71. In the longer term, the collaboration has carefully considered its options for relocating the experiment to achieve a 10% measurement of A_γ. Oak Ridge National Laboratory (ORNL) is a particularly attractive alternative to LANL by virtue of its two state-of-the-art neutron beam facilities – the upgraded High Flux Isotope Reactor (HFIR) which is currently in operation, and the Spallation Neutron Source (SNS), which is under construction. Both facilities would offer 1–2 orders of magnitude higher beam flux than is presently available at LANSCE. While HFIR management had initially offered to build a new cold neutron beam line to accommodate the NPDGamma experiment in the short term, the US DOE Office of Nuclear Physics has recently indicated a strong preference to relocate NPDGamma at the SNS as a high priority element of the SNS nuclear physics program [DOE Review of the NPDGamma Experiment, Los Alamos National Laboratory, October 5–7, 2004].

Collaborators (spokesman is underlined): M. Gericke, G. Hansen, M.B. Leuschner, B. Losowski, H. Nann, S. Santra, W.M. Snow (Indiana University); J.D. Bowman, G.S. Mitchell, S.I. Penttila, P.-N. Seo, W.S. Wilburn, V.W. Yuan (Los Alamos National Laboratory); R.D. Carlini (Thomas Jefferson National Accelerator Facility); T.E. Chupp, K.P. Coulter (University of Michigan); T.R. Gentile (National Institute of Standards and Technology); T. Case, S.J. Freedman, B. Lauss (University of California, Berkeley); T. Ino, S. Ishimoto, Y. Masuda (KEK National Laboratory, Japan); G.L. Jones (Hamilton College); M. Dabaghyan, F.W. Hersman, H. Zhu (University of New Hampshire); R.C. Gillis, S.A. Page, W.D. Ramsay (University of Manitoba); E.I. Sharapov (Joint Institute for Nuclear Research, Dubna); T.B. Smith (University of Dayton); D. Desai, G.L. Greene, R. Mahurin (University of Tennessee).